Published in final edited form as:
Biochem J. 2015 May 15; 468(1): 49–63. doi:10.1042/BJ20140697.

Inhibition of the malate-aspartate shuttle in mouse pancreatic islets abolishes glucagon secretion without affecting insulin secretion

Jelena A. Stamenkovic[*], **Lotta E. Andersson**[*], **Alice E. Adriaenssens**[†], **Annika Bagge**[*], **Vladimir V. Sharoyko**[*], **Fiona Gribble**[†], **Frank Reimann**[†], **Claes B. Wollheim**[‡,§], **Hindrik Mulder**[*], **Peter Spégel**[*,2]

[*]Unit of Molecular Metabolism, Department of Clinical Sciences in Malmö, Lund University Diabetes Centre, CRC, Lund University, Skåne University Hospital, Malmö, Sweden [†]MRC Metabolic Diseases Unit, Wellcome Trust-MRC Institute of Metabolic Sciences, Addenbrooke´s Hospital, Cambridge, United Kingdom [‡]Department of Clinical Sciences in Malmö, Lund University Diabetes Centre, CRC, Lund University, Skåne University Hospital, Malmö, Sweden [§]Department of Cell Physiology and Metabolism, University Medical Centre, 1 rue Michel-Servet, Geneva 4, Switzerland

Abstract

Altered secretion of insulin as well as glucagon has been implicated in the pathogenesis of Type 2 Diabetes, but the mechanisms controlling glucagon secretion from α-cells largely remain unresolved. Therefore, we studied the regulation of glucagon secretion from αTC1-6 cells and compared it to insulin release from INS-1 832/13 cells. We found that INS-1 832/13 and αTC1-6 cells, respectively, secreted insulin and glucagon concentration-dependently in response to glucose. In contrast, tight coupling of glycolytic and mitochondrial metabolism was observed only in INS-1 832/13 cells. While glycolytic metabolism was similar in the two cell-lines, Krebs-cycle metabolism, respiration and ATP-levels were less glucose-responsive in αTC1-6 cells. Inhibition of the malate-aspartate shuttle, using phenyl succinate, abolished glucose-provoked ATP production and hormone secretion from αTC1-6, but not INS-1 832/13 cells. Blocking the malate-aspartate shuttle increased levels of glycerol-3-phosphate only in INS-1 832/13 cells. Accordingly, relative expression of constituents in the glycerolphosphate shuttle compared to malate-aspartate shuttle was lower in αTC1-6 cells. Our data suggest that the glycerolphosphate shuttle augments the malate-aspartate shuttle in the INS-1 832/13 but not in αTC1-6 cells. These results were confirmed in mouse islets, where phenyl succinate abrogated secretion of glucagon but not insulin. Furthermore, expression of the rate-limiting enzyme of the glycerolphosphate shuttle, was higher in sorted primary ß- than α-cells. Thus, suppressed glycerolphosphate shuttle activity in the α-cell

[2]To whom correspondence should be addressed: Peter Spégel, Department of Clinical Sciences, Unit of Molecular Metabolism, Lund University Diabetes Centre, CRC, Scania University Hospital, 205 02 Malmö, Sweden, Tel.: +46 40 391009; peter.spegel@med.lu.se.

Author Contribution

JAS and LEA conducted functional assays, AB assisted in the OCR experiments, VVS assisted in the functional assays, AEA performed expression analyses, FR and FG oversaw expression analyses, CBW and HM assisted in writing of the manuscript. All authors contributed to analysis of the data. PS conceived the study, performed metabolomics analyses and finalized the manuscript.

Europe PMC Funders Author Manuscripts

may prevent a high rate of glycolysis and consequently glucagon secretion in response to glucose. Accordingly, pyruvate- and lactate-elicited glucagon secretion remains unaffected since their signaling is independent on mitochondrial shuttles.

Keywords

Cell metabolism; coupling factors; endocrinology; glucose metabolism; mitochondrial transport; islets; metabolomics; mass spectrometry; insulin; glucagon

Introduction

Type 2 Diabetes (T2D) results when an increasing demand for insulin is not met, frequently due to insulin resistance in an obese and/or sedentary individual [1]. Two main hormones control blood glucose levels: insulin, secreted from the ß-cell in response to hyperglycemia, and glucagon, secreted from the α-cell in response to hypoglycemia. Glucagon then acts mainly on the liver, whereas insulin also acts on peripheral target tissues to support anabolic and suppress catabolic metabolism [2,3]. Insufficient secretion of insulin is known to be associated with T2D, whereas a pathogenic role for the islet hormone glucagon in T2D has long been debated [4]. It has been suggested that abnormal control of glucagon secretion may contribute to hyperglycemia [5], a hallmark of diabetes. Importantly, deficient glucagon secretion in long-standing diabetes impairs the counter-regulatory response during hypoglycemia [5,6], the complication of insulin therapy most feared by patients.

Glucose is known to promote secretion of insulin and suppress secretion of glucagon *in vivo* and from isolated islets *in vitro*. It has therefore been assumed that stimulus-secretion coupling differs between α- and ß-cells. Studies on stimulus-secretion coupling in pancreatic ß-cells has implicated two pathways in the control of hormone secretion: the ATP-sensitive K^+ (K_{ATP})-channel dependent triggering pathway and the K_{ATP}-independent amplifying pathway [7]. The triggering pathway implies that increased glucose levels provoke augmented ATP-production, resulting in an increased ATP/ADP-ratio and closure of K_{ATP}-channels [8]. This causes plasma membrane depolarization, opening of voltage-sensitive Ca^{2+}-channels and release of insulin [9]. The triggering pathway is complemented by an amplifying pathway that augments insulin secretion in the presence of elevated levels of intracellular Ca^{2+}, critically depending on a rise in intra-mitochondrial Ca^{2+} [10]. The amplifying pathway has been suggested to involve, *e.g.*, NADPH [11,12] and glutamate [13–15] generated from glucose metabolism. However, only ATP has received undisputed support as a coupling factor in glucose-stimulated insulin secretion (GSIS) [16,17].

In contrast to the wealth of knowledge about stimulus-secretion coupling in ß-cells, the mechanism by which glucagon secretion is regulated is much less understood. A longstanding belief that α-cells sense glucose and regulate glucagon secretion in an inverse relationship has been challenged by the finding that isolated primary α-cells glucose dependently increase secretion of glucagon [18–20]. This, in turn, suggests a paracrine regulation of glucagon secretion *in vivo* [18–20]. Although the exact mechanism underlying this regulation remains incompletely understood, GABA, Zn^{2+} and insulin secreted from the pancreatic β-cells as well as somatostatin, secreted from pancreatic δ-cells, have been

Europe PMC Funders Author Manuscripts

suggested to underlie the paracrine regulation of glucagon secretion [18–23]. Although α- and ß-cells express the same K_{ATP}-channels the activity is lower in α-cells [24]. In ß-cells, Ca^{2+}-currents dominate electrophysiological activity during exocytosis [25]. In α-cells, although Ca^{2+}-current is detectable, it only comprises 15% of the magnitude of the Na^{+}-current [26,27]. In primary cultures and islets, it has been shown that α-cell Ca^{2+}-currents decrease in response to glucose stimulation; however the effects are minor [19,21]. The effect also appears to depend on co-localization with other cells within an islet as in dispersed sorted α-cells the opposite was true [18], blocking L-type Ca^{2+}-channels had little to no effect on glucagon secretion, while blocking P/Q-type channels decreased glucagon secretion [28,29]. In ß-cells, by contrast, blocking L-type channels abolished insulin secretion, while blocking P/Q-type channels appeared less important [30].

The relative hypersecretion of glucagon observed in diabetes [31] supports the notion that a deficient secretory response from the ß-cell may result in supranormal secretion of glucagon. Hence, in the absence of insulin, anabolic processes will remain inactive [2]. In addition, due to the associated lack of inhibitory effects of ß-cell secretory products, glucagon secretion will remain high and catabolic processes, such as hepatic glucose production, will remain active [3]. Overall, glucose consumption will be reduced and glucose production enhanced, resulting in increasing blood glucose levels. However, the significance of paracrine regulation of glucagon secretion has been challenged by the lack of correlation between somatostatin and insulin secretion with glucagon secretion [28,32]. Instead, glucose has been suggested to inhibit glucagon secretion directly [33], *via* modulation of K^{+}_{ATP}-channel activity [28].

Clearly, if stimulus-secretion coupling in α- and ß-cells is similar, the effect of potential drugs targeting insulin secretion *via* ß-cell metabolism, and other processes within its glucose-sensing machinery, are likely to also affect secretion of the counteractive hormone glucagon. Hence, identification of unique modulators of ß- and α-cell glucose sensing and secretory machinery could allow independent manipulation of either insulin or glucagon secretion with a view to influence glucose handling in the diabetic state.

Clearly, stimulus secretion coupling in the α-cell differs from that of the ß-cell but the nature of these differences is still unclear. In the present study, we focus on metabolic differences in the cell types, which are upstream of Ca^{2+}-regulation and exocytosis, to identify unique and shared functions in α- and ß-cell stimulus-secretion coupling. To this end, we found that glucose-stimulated glucagon secretion was highly dependent on a functional malate-aspartate shuttle. Conversely, stimulus-secretion coupling in ß-cells was less dependent on this shuttle, due to the compensatory action of the glycerol-phosphate shuttle. These results therefore explain the ability of ß-cells to maintain a high level of insulin secretion in the presence of a high glucose load. In contrast, α –cells are most active during catabolic states, such as muscle exercise and starvation [23], when they can utilize lactate or pyruvate, the metabolism of which does not need metabolite shuttling into the mitochondrion.

Experimental Procedures

Cell culture

αTC1 clone 6 (αTC1-6) cells (American Type Culture Collection, ATCC, Manassas, VA) were cultured in DMEM (Invitrogen Cat.No. 31600-034) containing 16.7mM glucose and supplemented with 10% fetal bovine serum, 100 U/ml penicillin, 100 μg/ml streptomycin, 15 mM HEPES, 0.1 mM non-essential amino acids (Invitrogen), 0.2% bovine serum albumin, 1.5 g/L sodium bicarbonate. INS-1 832/13 cells were grown in RPMI-1640 containing 11.1 mM glucose and supplemented with 10% fetal bovine serum, 10 mM HEPES, 2 mM glutamine, 1 mM sodium pyruvate and 50 μM ß-mercaptoethanol. Both cell lines were cultured at 37°C in a humidified atmosphere containing 5% CO_2.

Islet isolation

Male CH3/He mice (used for functional studies) or transgenic mice expressing the fluorescent protein, Venus, under the control of the proglucagon promoter on a C57B6-background (used for isolation of primary cells) were used for islet isolation [34]. The pancreas was injected immediately following cervical dislocation with collagenase V (0.5 mg/mL) in Ca^{2+} and Mg^{2+}-free HBSS. Pancreata were then dissected from the surrounding tissue and transported on ice. Following digestion at 37°C, the pancreas was disrupted by vigorous shaking, and the islets hand-picked under a stereo microscope. Islets used for functional studies recovered overnight in RPMI 1640 containing 5.5 mM glucose supplemented with 10% fetal bovine serum, 100 units/ml penicillin and 100 μg/ml streptomycin, at 37°C in a humidified atmosphere containing 5% CO2. Islets used for isolation of primary α- and ß-cells were disrupted into single cells by trituration following a 1 min incubation in Ca^{2+}-free HBSS containing 0.1x trypsin/EDTA and 0.1% FCS. Cells were immediately sorted by flow cytometry using a BD Influx cell sorter (BD Biosciences, San Jose, CA) equipped with a 488 laser for excitation of Venus. Venus-negative cells were further subdivided into a population that was large (according to side and forward scatter) and with high background auto-fluorescence at 530 and 580 nm. Cells were collected into RLT lysis buffer (Qiagen, UK) and frozen on dry ice.

Hormone secretion

INS-1 832/13 and α-TC1-6 cells were seeded in 24-well tissue culture plates and cultured over night. The following day, αTC1-6 cells were pre-incubated in HEPES balanced salt solution (HBSS; 114 mM NaCl, 4.7 mM KCl, 1.2 mM KH_2PO_4, 1.16 mM $MgSO_4$, 20 mM HEPES, 2.5 mM $CaCl_2$, 25.5 mM $NaHCO_3$, 0.2% BSA, pH 7.2) supplemented with 5.5 mM glucose for 2 h at 37°C with 5% CO_2. INS-1 832/13 cells were pre-incubated for 2 h in HBSS supplemented with 2.8 mM glucose. Following the pre-incubation, αTC1-6 cells were incubated for 1 h in HBSS containing either 1 mM glucose or 16.7 mM glucose in presence or absence of 10 mM phenylsuccinate. INS-1 832/13 cells were incubated in HBSS containing either 2.8 mM glucose or 16.7 mM glucose, in the presence or absence of 10 mM phenylsuccinate. Secreted glucagon and insulin were measured by a glucagon RIA (Millipore, Billerica, MA) or the Coat-a-Count insulin RIA (Siemens Medical Solutions Diagnostics, Los Angeles, CA), according to the manufacturer's instructions. Finally, cells were washed in PBS, lysed by addition of 50 μl of lysis buffer (50 mM Tris, 200 mM NaCl,

2 mM EDTA, 1% Triton-X100, pH 7.4) and protein content determined using the bicinchoninic acid protein assay (BCA Protein Assay kit, Thermo Fisher Sientific).

Mouse islets (n=4) were pre-incubated in Krebs-Ringer bicarbonate buffer (KRB; 115 mM NaCl, 4.7 mM KCl, 2.6 mM $CaCl_2$, 1.2 mM $MgSO_4$, 20 mM $NaHCO_3$, and 16 mM HEPES) containing 0.2 % BSA and 2.8 mM glucose for 1 h, followed by exchange of buffer to KRB containing 2.8 mM glucose or 16.7 mM glucose with or without 10 mM phenylsuccinate for 1 h. Secreted glucagon and insulin were assayed using the Mercodia Glucagon and Insulin ELISA (Mercodia, Uppsala, Sweden), respectively.

Metabolite profiling

Metabolite profiling was performed in αTC1-6 and INS-1 832/13 cells as previously described in detail [35,36]. In brief, α-TC1-6 and INS-1 832/13 cells were seeded in 12-well and 24-well plates, respectively, and treated as described for hormone secretion. After the final incubation, cells were swiftly washed with 1 mL of ice-cold PBS and metabolism quenched by addition of 300 μL methanol at -80°C. Cells were scraped off and metabolites extracted using a one-phase liquid extraction protocol [35]. Metabolites were derivatized and analyzed on a gas chromatograph (GC; Agilent 6890N, Agilent Technologies, Atlanta, GA) connected to a time-of-flight mass spectrometer (TOF-MS; Leco Pegasus III TOFMS, Leco Corp., St. Joseph, MI). Data were acquired using Leco ChromaTof (Leco Corp.), exported as NetCDF files, and processed using hierarchal multivariate curve resolution (HMCR) [37] in MATLAB 7.0 (Mathworks, Natick, MA).

Plasma membrane potential and cytoplasmic free Ca^{2+}

Cells were seeded onto Poly-D-lysine coated 8-well chambered cover glasses (Lab-Tek, Naperville, IL) and cultured for 48 hours prior to analysis. On the day of analysis the cells were incubated in 400 μl of buffer P (135 mM NaCl, 3.6 mM KCl, 1.5 mM $CaCl_2$, 0.5 mM $MgSO_4$, 0.5 mM Na_2HPO_4, 10 mM HEPES, 5 mM $NaHCO_3$, pH 7.4) containing 2.8 mM glucose for 90 minutes at which 0.2 μM Fluo-4 AM (Invitrogen, Life Technologies, Carlsbad, CA), 0.25 mM sulfinpyrazone (a multi-specific inhibitor of organic anion transporters) and BSA (0.1%) were added and the incubation was continued for a further 30 minutes. A vial from a FLIPR® membrane potential assay kit, explorer format component A, containing a proprietary plasma membrane potential ($\Delta\psi_p$) indicator ("PMPI") (R-8042; Molecular Devices, Sunnydale, CA) was reconstituted in 10 ml water, and the buffer P containing Fluo-4 was removed and replaced with 400 μl fresh buffer P containing 4 μl PMPI immediately prior to imaging as described previously [38,39]. Excitation was performed at 488 nm (Flou-4) and 514 nm (PMPI) and emission recorded with a 530 nm long-pass filter [39] on a Zeiss LSM510 inverted confocal fluorescence microscope. Glucose was added to a final concentration of 2.8 mM, and then 16.7 mM, followed by addition of oligomycin (final concentration 0.5 μg/mL) and finally KCl (final concentration 25 mM). Traces were displayed in arbitrary fluorescent units.

RNA isolation and Quantitative real-time PCR

Total RNA was extracted from αTC1-6 and INS-1 832/13 cells using RNAeasy RNA purification kit (Qiagen GmbH, Hilden, Germany). RNA concentrations were determined

using a NanoDrop Spectrophotometer (Thermo Scientific). Equal quantities of total RNA were reverse transcribed using RevertAid™First-Strand cDNA synthesis kit (Fermentas, Vilnius, Lithuania) or Superscript III (Life Technologies) in reactions containing 500 ng or 1000 ng of total RNA. Quantitative real-time PCR (Q-PCR) was performed with 7900 HT Fast Real-Time PCR system (Applied Biosystems). The PCR reaction mix consisted of first-strand cDNA template, primer pairs (for details, see supplementary table 1), 6-carboxyfluorescein/quencher probes (Bioresearch Technologies, CA and Applied Biosystems), and PCR Master mix (Applied Biosystems) and was carried out as previously described [40]. Expression of selected targets was compared with that of hypoxanthine-guanine phosphoribosyl transferase (*Hprt*) measured on the same sample in parallel on the same plate, using the comparative Ct method.

Glucose utilization

INS-1 832/13 and αTC1-6 cells were seeded in 24-well tissue-culture plates and cultured overnight. Prior to assay, cells were washed in PBS and pre-incubated as described for hormone secretion. Then, the buffer was removed and 500 μl of HBSS containing D-[5-^{3}H] glucose (specific activity 19.63 Ci/mmol; Perkin Elmer Life Science) and glucose added to reach the same concentrations as were used for determination of hormone secretion. Subsequently, cells were incubated for 30 min at 37°C, followed by addition of 100 μl of 10% trichloracetic acid to prevent further metabolism of D-[5-^{3}H] glucose. The cells were harvested from the wells and 500 μl lysate transferred to 1.5 ml eppendorf tubes. The tubes were placed inside sealed scintillation vials, containing 500 μl of water and incubated at 56°C overnight to permit $^{3}H_2O$ formed by the cells to evaporate and equilibrate with water in the vials. The vials were cooled to room temperature and ^{3}H content in the water measured by liquid scintillation spectrometry [41]. Glucose utilization was calculated as previously described in detail [42].

Respiration

Cellular and mitochondrial oxygen consumption rate (OCR) was determined in αTC1-6 and INS-1 832/13 cells, using the Seahorse Extracellular Flux Analyzer XF24 (Seahorse Bioscience, Billerica, MA) as previously described in detail [42]. Prior to assay, cells were incubated for 2 h at 37°C in 750 μl assay medium containing 1 mM glucose and 2.8 mM glucose for αTC1-6 and INS-1 832/13 cells, respectively. OCR was then recorded in intact cells in the presence of 1 mM glucose (αTC1-6), 2.8 mM glucose (INS-1 832/13), 16.7 mM glucose or 10 mM pyruvate.

Lactate production

INS-1 832/13 and αTC1-6 cells were seeded in 24-well tissue culture plates and cultured and incubated as described for hormone secretion. Released lactate was determined in the supernatant by a colorimetric assay at 570 nm (Biovision, Milpitas, CA). The rate of lactate release was determined from a standard curve calculated from freshly prepared lactate solutions.

ATP measurement

INS-1 832/13 and αTC1-6 cells were seeded in 24-well plates and cultured overnight. Then, αTC1-6 cells were pre-incubated in HBSS containing 5.5 mM glucose for 2h, followed by 15 min incubation in HBSS containing 1 or 16.7 mM glucose in the presence or absence of 10 mM phenylsuccinate. INS-1 832/13 cells were pre-incubated in HBSS containing 2.8 mM glucose and finally incubated in HBSS containing either 2.8 mM glucose or 16.7 mM glucose, in the presence or absence of 10 mM phenylsuccinate. Subsequently, the incubation medium was removed, cells washed in PBS and lysed by addition of 100 ul of lysis buffer. Finally, cells were snap frozen on dry-ice/ethanol and ATP measured with a Luciferase-based luminescence assay (BioThema, Handen, Sweden) according to the manufacturer's instructions.

Statistical analysis

Statistical differences were assessed by the paired (within cell line) and unpaired (between cell lines) Student's t-test or one-way ANOVA followed by the Newman-Keuls multiple correction method *post hoc* when more than two groups were compared. Metabolite profiling data were analyzed in Simca P^+ 12.0 (Umetrics, Umeå, Sweden) using orthogonal projections to latent structures discriminant analysis (OPLS-DA) [43] on mean-centered and unit-variance scaled data.

Results

Glucose stimulates hormone secretion from αTC1-6 and INS-1 832/13 cells

First, we found that glucose concentration-dependently provoked secretion of glucagon (Figure 1A) and insulin (Figure 1B) from αTC1-6 and INS-1 832/13 cells, respectively. Glucagon secretion was elevated 2.0-fold at 16.7 mM glucose ($p<0.05$), compared to secretion at 1 mM glucose ($p<0.05$). Insulin secretion was elevated 1.1-fold ($p<0.05$) at 5.5 mM glucose and 3.8-fold ($p<0.01$) at 16.7 mM glucose, compared to insulin secretion at 2.8 mM glucose.

Metabolite profiling of INS-1 832/13 and αTC1-6 cells reveal differences in the coupling of cytosolic and mitochondrial metabolism

Glucose metabolism plays a key role in ß-cell stimulus-secretion coupling. To investigate whether this is the case also in α-cells, we investigated glucose-provoked alterations in glucose metabolism in αTC1-6 cells and compared it to that in INS-1 832/13 cells. Data generated from these two cell lines were normalized to baseline levels (1 mM glucose for αTC1-6 and 2.8 mM glucose for INS-1 832/13) and analyzed by OPLS-DA, using cell-type and glucose level as discriminating variables (2 predictive and 3 orthogonal components, $R^2_{(X)}=0.682$, $Q^2_{(Y)}=0.667$). Thereby, alterations in levels of metabolites provoked by glucose and differences in these between αTC1-6 and INS-1 832/13 cells could be detected. In the OPLS-DA score-scatter plot (Figure 2A) each data point represents a biological replicate with the position determined by levels of all 58 metabolites detected in both cell-types. It revealed a clear discrimination between αTC1-6 and INS-1 832/13 cells stimulated with 16.7 mM glucose.

To unravel the metabolic differences underlying the clustering observed in the score-scatter plot, the loading plot for the predictive components was examined (Figure 2B). This plot revealed that glucose provoked elevated levels of glycolytic- and tricarboxylic acid (TCA)-cycle intermediates in both cell lines. However, glucose-provoked elevation of TCA-cycle intermediates was much more pronounced in the INS-1 832/13-cells; alterations in glycolytic intermediates were more similar. Levels of glycerol-3-phosphate and glutamate increased while levels of aspartate decreased.

Next, the glucose-provoked fold-change in levels of glycolytic and TCA-cycle intermediates and metabolites involved in mitochondrial shuttling were examined (Figure 2C). Stimulation of cells with 16.7 mM glucose provoked a 3.7-fold ($p<0.05$) and 8.6-fold ($p<0.01$) increase in glucose-6-phosphate, a 1.9-fold ($p<0.05$) and 7.4-fold ($p<0.01$) increase in fructose-6-phosphate, a 1.6-fold ($p<0.01$) and 3.4-fold ($p<0.01$) increase in 3-phosphoglycerate and a 1.1-fold ($p<0.05$) and 1.8-fold ($p<0.001$) increase in alanine, in αTC1-6 and INS-1 832/13 cells, respectively. Hence, glucose elicited a significantly larger response in levels of fructose-6-phosphate (4.0-fold, $p<0.01$), 3-phosphoglycerate (2.1-fold, $p<0.001$), and alanine (1.6-fold, $p<0.001$), in the INS-1 832/13-cells compared to the αTC1-6 cells. Dihydroxyacetone phosphate levels increased 2.5-fold ($p<0.01$) in the α-TC1-6 cells, whereas they trended towards a glucose-stimulated elevation in INS-1 832/13 cells (3.3-fold, $p=0.078$). Among the TCA-cycle intermediates, levels of citrate increased 1.8-fold ($p<0.001$) and 6.1-fold ($p<0.01$), levels of fumarate increased 1.3-fold ($p<0.05$) and 3.0-fold ($p<0.05$), and levels of malate increased 1.7-fold ($p<0.01$) and 17-fold ($p<0.001$) in αTC1-6 and INS-1 832/13 cells, respectively. The glucose elicited elevation of levels of citrate was 3.5-fold ($p<0.001$), fumarate was 2.3-fold ($p<0.01$) and malate was 10.1-fold ($p<0.001$) higher in INS-1 832/13 cells compared to αTC1-6 cells. Levels of isocitrate (6.2-fold, $p<0.01$), α-ketoglutarate (8.7-fold, $p<0.001$), and succinate (1.7-fold, $p<0.001$), increased only in INS-1 832/13 cells. Hence, the response in levels of all detected TCA-cycle intermediates to glucose stimulation was higher in INS-1 832/13 cells compared to αTC1-6 cells. Levels of aspartate decreased 1.3-fold ($p<0.01$) and 3.5-fold ($p<0.001$), whereas levels of glutamate increased 1.5-fold ($p<0.001$) and 1.8-fold ($p<0.001$) in αTC1-6 and INS-1 832/13 cells, respectively. Levels of glycerol-3-phosphate increased 1.2-fold ($p<0.01$) in αTC1-6 cells and 1.3-fold ($p<0.01$) in INS-1 832/13-cells. Glucose-provoked elevation of glutamate and glycerol-3-phosphate levels did not differ between cell lines, although glucose-evoked reduction in aspartate levels was 2.7-fold ($p<0.001$) more efficient in the INS-1 832/13 cells than in the αTC1-6 cells.

Glycolytic rate is similar in αTC1-6 and INS-1 832/13 cells while mitochondrial metabolism is much less active in αTC1-6 cells

Thus, metabolite profiling revealed that the TCA-cycle was less glucose-responsive in the αTC1-6 compared to the INS-1 832/13 cell line. However, metabolite profiling in this way assesses accumulative levels of metabolites and does not allow firm conclusions regarding the underlying flux changes in the pathways the metabolites participate in. Although a difference is observed, we do not know whether this is due to altered flux or accumulation of metabolites. Therefore we investigated glycolytic rate in αTC1-6 and INS-1 832/13 cells, determined from the rate of [^{3}H]OH production from D-[5-^{3}H] glucose; one molecule of

[^{3}H]OH is formed when 2-phosphoglycerate is converted to phosphoenolpyruvate by enolase. Stimulation of αTC1-6 and INS-1 832/13 cells with 16.7 mM glucose caused a 3.5-fold ($p<0.05$) and a 4.3-fold ($p<0.01$) (Figure 3A) increase in glucose utilization, respectively. Neither basal, glucose-stimulated nor the fold-change in glucose utilization differed between αTC1-6 and INS-1 832/13 cells.

Next, we investigated mitochondrial metabolism, which plays a pivotal role in ß-cell stimulus-secretion coupling. To this end, we could show that O_2-consumption, a measure of mitochondrial metabolism reflecting respiratory chain activity, was highly glucose- and pyruvate-responsive in the INS-1 832/13 cells. Respiration in the presence of 16.7 mM glucose or 10 mM pyruvate was 1.3-fold ($p<0.001$) and 1.25-fold ($p<0.001$), respectively, compared to respiration at 2.8 mM glucose (Figure 3B). The rate of respiration in presence of these nutrients was much less pronounced in the αTC1-6 cells; glucose was ineffective in increasing respiration whereas pyruvate-provoked a 1.1-fold ($p<0.05$) increase in respiration (Figure 3B). Hence, results from measurement of glucose- and pyruvate-stimulated O_2-consumption supports the idea that the greater accumulation of citric acid cycle intermediates reflects greater Krebs cycle activity in INS-1 832/13 cells.

The relative contribution of aerobic and anaerobic metabolism differs between INS-1 832/13 and αTC1-6-cells

The ultimate product of aerobic metabolism, reflected by the OCR, is the triggering signal of GSIS, *i.e.* ATP. Hence, we assessed levels of ATP after stimulation of INS-1 832/13 and αTC1-6 cells with glucose. Levels of ATP increased 1.5-fold ($p<0.01$) in INS-1 832/13 cells stimulated with 16.7 mM glucose, compared to 2.8 mM glucose (Figure 4A). Changes in ATP-levels in αTC1-6 cells stimulated with 16.7 mM glucose were much less pronounced; levels of ATP trended to an increase (1.1-fold, $p=0.11$) in αTC1-6 cells stimulated with 16.7 mM glucose, compared to cells stimulated with 1 mM glucose (Figure 4A).

Whereas marked differences in mitochondrial metabolism were observed between INS-1 832/13 cells and αTC1-6 cells, differences in glycolytic metabolism were much less pronounced. Regeneration of cytosolic NAD^+ is critical to maintain a high glycolytic rate. In situations where mitochondrial respiration is low this may be conferred by lactate dehydrogenase (LDH), reducing pyruvate to lactate. At basal glucose levels, significant amounts of lactate were released from the αTC1-6 cells, whereas lactate release was not detected from INS-1 832/13 cells (Figure 4B). Stimulation of cells with 16.7 mM glucose did not affect lactate release from the αTC1-6 cells, whereas marked release of lactate was detected from the INS-1 832/13 cells (Figure 4B).

The mitochondrial fuel pyruvate increased OCR, whereas glucose was largely inefficient in doing so in the αTC1-6 cells. Hence, if metabolism controls glucagon secretion, then pyruvate may be more efficient in stimulating glucagon secretion. Stimulation of cells with 10 mM pyruvate provoked a 14% ($p<0.05$) greater increase in glucagon secretion from αTC1-6 cells, compared to 16.7 mM glucose (Figure 4C). In the INS-1 832/13-cells, on the other hand, insulin secretion evoked by 10 mM pyruvate was similar to insulin secretion evoked by 16.7 mM glucose (Figure 4C).

Plasma membrane potential and cytoplasmic free Ca^{2+}

Synchronized oscillations in Ca^{2+} and plasma membrane potential are hallmarks of ß-cell hormone exocytosis. We found a 3.6 fold ($p<0.05$) increase in magnitude of oscillations in the cytoplasmic free Ca^{2+} and a 5.6 fold ($p<0.05$) increase in the amplitude of the plasma membrane potential oscillations in the INS-1 832/13 cells (Figure 5A-B). Glucose evoked neither a change in Fluo-4 nor PMPI fluorescence, suggesting that glucose does not affect plasma membrane potential or cytosolic calcium (Figure 5A-B).

Inhibition of the 2-oxoglutarate carrier reduces insulin secretion from INS-1 832/13 cells and abolishes glucose-stimulated glucagon secretion from αTC1-6 cells

So far, we have found that glycolytic rate was similar in INS-1 832/13 and αTC1-6 cells, whereas pronounced differences were observed in mitochondrial metabolism. No difference was observed in lactate secretion, whereas metabolite profiling data revealed similar responses in levels of intermediates involved in mitochondrial shuttles in both cell lines. Hormone secretion from the αTC1-6 cells was more potently increased in response to the mitochondrial fuel pyruvate, whereas insulin secretion in presence of 16.7 mM glucose or 10 mM pyruvate did not differ. These data suggest that mitochondrial shuttling may be limiting secretion of glucagon in response to glucose. Therefore, we further investigated the impact of mitochondrial shuttles on hormone secretion by inhibiting the mitochondrial 2-oxoglutarate carrier, an integral part of the malate-aspartate shuttle, with 10 mM phenylsuccinate. Glucagon secretion from the αTC1-6 cells was reduced by 35% ($p<0.05$; Figure 6A) in presence of 10 mM phenylsuccinate. As a result, glucose-provoked glucagon secretion was completely abolished. Insulin secretion from INS-1 832/13 cells was reduced by 30% ($p<0.05$; Figure 6A). Hence, in presence of 10 mM phenylsuccinate, 16.7 mM glucose still provoked a 4.2-fold ($p<0.001$) increase in insulin secretion, compared to 2.8 mM glucose.

Metabolite profiling after addition of phenylsuccinate revealed a concurrent reduction in levels of glutamate. Glucose-provoked glutamate production was almost completely abolished (-29%, $p<0.001$) in the αTC1-6 cells and largely reduced (-23%, $p<0.05$) in the INS-1 832/13 cells (Figure 6B). Glucose-provoked suppression of aspartate levels was unaffected by phenylsuccinate in both cell lines. Glucose-elicited production of glycerol-3-phosphate, an intermediate of the glycerolphosphate shuttle, was abolished in the αTC1-6 cells (-33%, $p<0.01$) and potentiated in the INS-1 832/13 cells (1.9-fold, $p<0.01$). Reduction of pyruvate to lactate by LDH could potentially compensate for the loss of malate-aspartate shuttle activity. However, lactate release from both αTC1-6 and INS-1 832/13 cells was reduced by 35% ($p<0.05$) and 79% ($p<0.001$), respectively, in the presence of 10 mM phenylsuccinate (Figure 7A).

Thus, our data show that the impact of phenylsuccinate on hormone secretion and shuttle-activity differed between the αTC1-6 and INS-1 832/13 cell lines. Clearly, this implies that mitochondrial metabolism also will be impacted. To investigate this, we monitored the effect of phenylsuccinate on cellular levels of ATP. At 16.7 mM glucose in the presence of 10 mM phenylsuccinate, ATP levels were reduced by 10% ($p<0.05$; Figure 7B) in αTC1-6 cells,

thereby completely abolishing glucose-provoked ATP-production. Conversely, levels of ATP in INS-1 832/13-cells were unaltered by phenylsuccinate (Figure 7B).

Inhibition of the 2-oxoglutarate carrier abolishes glucagon secretion but has no effect on Insulin secretion from isolated mouse islets

To verify our results from studies in clonal cell lines, we measured secretion of insulin and glucagon after stimulation of mouse islets with 16.7 mM glucose in presence or absence of 10 mM phenylsuccinate (Figure 9). Glucose was found to provoke a 4.4-fold ($p<0.001$) increase in insulin secretion and a 54% ($p<0.05$) reduction in glucagon secretion. In contrast, phenylsuccinate did not affect GSIS, while secretion of glucagon was abolished (-94%, $p<0.05$) in presence of this inhibitor of the mitochondrial 2-oxoglutarate carrier.

Expression of components of the glycerolphosphate-and malate-aspartate-shuttles in αTC1-6 cells, INS-1 832/13 cells and sorted primary α- and ß-cells

Taken together, our results suggest an essential role of the malate-aspartate shuttle in glucose-stimulated glucagon secretion from αTC1-6 cells. A loss of malate-aspartate shuttle activity in the INS-1 832/13 cells may be compensated for by an increased activity in the glycerolphosphate shuttle. We therefore examined gene expression of key enzymes of the malate-aspartate- and glycerolphosphate-shuttles (Figure 9). Expression of the mitochondrial aspartate/glutamate carrier (*Agc1*; *Aralar1*, *Slc25a12*) was 12.5-fold ($p<0.01$) higher in αTC1-6 than in INS-1 832/13 cells. The cytosolic glycerol-3-phosphate dehydrogenase (*Gpd1*) was expressed markedly higher in INS-1 832/13 compared to αTC1-6 cells (7800-fold, $p<0.001$). The ratio of expression of mitochondrial glycerol-3-phosphate dehydrogenase (*Gpd2*) to *Agc1* and the cytosolic aspartate amino transferase (*Got1*) was 40-fold ($p<0.001$) and 5.2-fold ($p<0.01$) higher in INS-1 832/13 compared to αTC1-6 cells. Expression of *Got1* (1.7-fold, $p<0.05$) and *Gpd2* (2.1-fold, $p<0.05$) was higher in primary ß-cells, compared to α-cells. Hexokinase 2 (*Hk2*) expression was detected only in αTC1-6. mRNA for the liver isoform of pyruvate kinase (*Pklr*) was only detected in primary cells, whereas the muscle isoform (*Pkm2*) was expressed at much higher levels in in INS-1 832/13 (70- to 400-fold, $p<0.001$) than in the αTC1-6 and the primary α- and ß-cells.

Discussion

Despite the inappropriate, and potentially harmful, hypersecretion of glucagon observed in T2D [31], few studies have investigated stimulus-secretion coupling in the α-cell [23]. To some extent this may be explained by the low fraction of α-cells in the islet. The islet contains 20-40% α-cells, whereas it contains as much as 60-80% ß-cells [44]. Consequently, the islet has since long been used as a model for the ß-cell. Knowledge on stimulus-secretion coupling in α-cells was until recently obscured by the *in vivo* observations of decreased glucagon secretion with increasing blood glucose levels. Clearly, recent studies, showing that *in vitro* purified α-cells increase secretion of glucagon with increasing glucose concentrations, have challenged the established paradigm of α-cell stimulus-secretion coupling [18–20]. Thus, α-cells isolated from their natural environment respond to glucose in a manner qualitatively similar to that of the ß-cell. Hence, factors secreted from neighboring endocrine cells *in vivo*, such as insulin, zinc and GABA, have been suggested to

suppress glucagon secretion *in vivo* [18–23]. Importantly, glucagon secretion from dispersed islet cells was suppressed by glucose, whereas the opposite occurred when non-α-cells were removed [20].

Due to the difficulties in isolating sufficient amounts of primary α-cells for multiple experiments, including metabolite profiling, we investigated the clonal glucagon-secreting cell line αTC1-6 as an α-cell model. Of the glucagon-producing cell lines, the αTC1-6 cell line exhibits the most differentiated α-cell phenotype; it does not produce insulin, somatostatin or pancreatic polypeptide, and expresses higher levels of glucagon than αTC1 and αTC1-9 [45]. We therefore compared results from this cell line with results derived from a well-characterized rat ß-cell line (INS-1 832/13) [46].

Indeed, we verified that the clonal αTC1-6 cell line responds similarly to glucose stimulation as primary sorted α-cells, *i.e.*, with increased glucagon secretion [18–20]. Hence, the αTC1-6 and INS-1 832/13 cell lines both responded with increased hormone secretion to elevated glucose levels. While the qualitative responses in levels of metabolites in central glucose metabolism to glucose stimulation were largely similar between these cell lines, several noteworthy quantitative differences were found. Thus, glycolytic metabolism responded similarly to glucose stimulation in the two cell lines, but glucose-provoked alterations in the TCA-cycle were much less pronounced in the αTC1-6 cell line. This was associated with similar glucose utilization in both cell lines. However, whereas mitochondrial metabolism and ATP-production were highly glucose-responsive in the INS-1 832/13 cells, these responses were largely glucose-unresponsive in the αTC1-6 cell line. Notably, the mitochondrial substrate pyruvate was more efficient than glucose in provoking glucagon secretion from the αTC1-6 cells; this coincided with a minor, albeit significant, increase in OCR also observed in the αTC1-6 cells. These results confirm findings from primary islet cells in which glucose-provoked ATP [22,47] and FADH2 production [48] have been shown to be lower in the α-cell than in the ß-cell. Overall, our findings of less efficient coupling of glycolysis and TCA-cycle metabolism in the αTC1-6 cell line support other studies in which mitochondrial metabolism has been shown to be significantly more glucose-responsive in the ß-cell [22,23,49]. In fact, we have previously demonstrated that a tight coupling of glycolytic to mitochondrial metabolism is hallmark of robust insulin secretion in clonal ß-cells [42]. In line with this, the inefficient coupling of glycolytic and mitochondrial metabolism observed in the αTC1-6 cells paralleled the low fold-change in glucose-stimulated glucagon secretion, as opposed to the more efficient coupling and more robust response in insulin secretion observed in the INS-1 832/13 cells.

Notably, we found that stimulation of αTC1-6 and INS-1 832/13 cells with glucose provoked increased levels of glutamate and glycerol-3-phosphate and decreased levels of aspartate, confirming previous findings in the INS-1 832/13 cell line [36]. These intermediates are all part of the mitochondrial shuttles. This, together with a similar release of lactate, indicates that mitochondrial shuttling, which has been shown to be of paramount importance in ß-cell stimulus-secretion coupling [50,51], maintained a high glycolytic rate also in the αTC1-6 cell line.

To investigate the importance of mitochondrial shuttling in stimulus-secretion coupling in the αTC1-6 and the INS-1 832/13 cell lines, we inhibited the 2-oxoglutarate transporter, using phenylsuccinate [52]. Interestingly, whereas this inhibitor only attenuated GSIS from the INS-1 832/13 cell line, it completely abolished glucose-stimulated glucagon secretion from the αTC1-6 cell line. Hence, our data confirm previous findings of reduced insulin secretion with the pharmacological inhibitor in purified rat ß-cells [14] as well as with results from INS-1 832/13 cells and rat islets in which the 2-oxoglutarate transporter has been silenced [53]. Glucose-provoked glutamate production, respiration and ATP-production were concurrently abolished in the αTC1-6 cells, whereas only a slight decrease in glutamate levels was observed in the INS-1 832/13 cells. The reduction in levels of glutamate was paralleled by increased levels of glycerol-3-phosphate only in the INS-1 832/13-cells. Hence, these data suggest that the glycerolphosphate shuttle compensated for the loss of malate-aspartate shuttle activity only in the INS-1 832/13-cell. Notably, cellular release of lactate, reflecting anaerobic replenishment of cytosolic NAD^+, did not compensate for loss of malate-aspartate-shuttle activity neither in the αTC1-6 nor the INS-1 832/13 cell line. Although expression of both LDH and MCT1 is low in primary ß-cells [54,55], sorted primary ß-cells have been shown to release lactate when stimulated with glucose [54]. Importantly, we also showed that phenylsuccinate was without effect on insulin secretion from isolated mouse islets, whereas glucagon secretion was completely abolished.

Mitochondrial metabolism in the ß-cell has been suggested to be supply- rather than demand-driven, implicating a complete oxidation of glucose in glycolysis and the TCA-cycle [56]. To maintain a high glycolytic flux, efficient shuttling of NADH from the cytosol to the mitochondria is required. Our results support previous findings implicating mitochondrial shuttles in GSIS [50,51,57]. Furthermore, it has also been shown that the glycerolphosphate shuttle and the malate-aspartate-shuttle compensate for each other and that both shuttles need to be inhibited to impair glucose oxidation and insulin secretion from pancreatic islets [51]. A lower expression of *Gpdh2* in the α-cell agrees with our findings of a compensatory activity of the glycerolphosphate shuttle only in the ß-cell. Our results therefore confirm previous studies in which protein expression and activity of GPD2 have been shown to be similar in primary sorted ß-cells and the INS-1 cell line, being about 10-fold higher in these cells compared to islet non-ß-cells [54]. Furthermore, expression of *Gpd2* has previously been studied in conjunction with the β-cell ”disallowed” gene *Ldh* [58]; the ratio of *Gpdh2*-to-*Ldh* was found to be 2-3 orders of magnitude greater in primary ß-cells and INS-1 cells, compared to other islet cells [54]. Moreover, impairments in the glycerolphosphate shuttle have been observed in animal models of T2D [59,60] and in T-lymphocytes from T2D patients [61].

The glycerolphosphate shuttle is expressed in metabolically highly active tissues, such as brown fat and ß-cells [54,62,63]. One reason for its limited expression is the energy loss resulting from the conversion of NADH to $FADH_2$; this energy is converted into heat [64]. The energy loss has been suggested to allow this shuttle to transfer electrons against an unfavorable electron gradient, *i.e.*, this shuttle is functional even in situations with high mitochondrial NADH-levels. In contrast, activity in the malate-aspartate shuttle does not result in any loss of energy. In brown adipose tissue, a high rate of fuel oxidation is required to generate heat [64]. Likewise, in the ß-cell, the glycerolphosphate shuttle allows a high

glycolytic rate even in situations when the mitochondrial redox-potential is very high; this would extend the range of glucose concentrations at which insulin can be concentration-dependently secreted. Reduced expression of this shuttle in the α-cell may therefore prevent hypersecretion of glucagon at hyperglycemia.

Pyruvate and lactate have also been suggested to be important α-cell secretagogues [22,65]. Levels of these metabolites increase in the blood during exercise [66], when glucose is mobilized from liver. As these metabolites enter glycolysis down-stream of glyceraldehyde 3-phosphate dehydrogenase they do not generate glycolytic NADH (or consume NAD^+) and therefore do not rely on mitochondrial shuttles. Hence, the lack of glycerolphosphate shuttle activity in the α-cell may divert nutrient sensing from glucose to substrates available in situations where secretion of glucagon is warranted. The finding that mitochondrial nutrients provoked a similar increase in ATP-production in α- and ß-cells, whereas glucose provoked ATP-production is much less efficient in the α-cell is in support of this [22].

Notwithstanding the observed alterations in intermediates involved in mitochondrial shuttles, glutamate is also a suggested coupling factor in GSIS [13,14,67], although this hypothesis has also been challenged [68]. Here, we observed reduced levels of glutamate paralleling reduced GSIS in the INS-1 832/13-cells. Notably, this occured without effects on the main trigger of insulin secretion, *i.e.*, ATP. In the αTC1-6, a more dramatic reduction in glucagon secretion and glutamate levels was observed, but this coincided with abolished ATP-production. In a previous study, suppression of glutamate production, using phenylsuccinate, and glutamate release [14], using L-trans-pyrrolidine-2,4-dicarboxylate (tPDC), was found not to affect glucagon secretion from sorted α-cells [14]. However, in the same study epinephrine, which also reduces glutamate release, as does tPDC, potentiates glucose-stimulated glucagon release. Expression of *Pklr* in the primary cells may suggest this effect to be due to activation of glycolysis; *Pkm* is unaffected by epinephrine. In contrast to our present results, exposure to 10 mM phenyl succinate for 30 minutes has previously been shown to inhibit insulin secretion from sorted primary ß-cells, while lacking effects on glucagon secretion from sorted primary α-cells [14]. It should be borne in mind that cell-cell communication is disrupted when islet cells are dissociated [69]. This is not the case in the present study, where intact islets or confluent cell cultures were used. Furthermore, cellular function may also be influenced by the stress caused by the relatively rough treatment required for islet cell dissociation. In our experiments, not only hormone secretion, but also cellular metabolism, reacted similarly to addition of phenyl succinate in α- and ß-cells, respectively. Clearly, the role of glutamate as a coupling factor in α-cell stimulus-secretion coupling needs further investigation.

It must be noted that the detailed examination of metabolism in the α- and ß-cells conducted here were mainly performed in cell-models. Clearly, expression of metabolic enzymes differ between the clonal cell-lines and their primary counterparts [70], as evident from altered expression of *Hk* and *Pk* isoforms shown here. A disadvantage of using phenylsuccinate is that chemical inhibitors rarely are perfectly selective, which would call for the use of gene-silencing techniques. Phenylsuccinate has also been suggested to inhibit the dicarboxylate carrier, which is involved in shuttling of malate and succinate across the mitochondrial membrane [71]. However, silencing of genes is also likely to cause compensatory effects in

the metabolic network. Thus, silencing may be more useful in studies of chronic effects, than to resolve acute effects related to stimulus-secretion coupling. Here, we show that phenylsuccinate indeed affects levels of constituents of the malate-aspartate shuttle. Hence, independent of whether these changes are the result of altered shuttle activity or any other metabolic reaction, changes in levels of glutamate will affect the equilibrium of this shuttle, as has been suggested in heart muscle [72]. Importantly, in the presence of phenylsuccinate, the INS-1 832/13 cells, which express the glycerolphosphate shuttle, compensated by increasing levels of glycerol-3-phosphate. Hence, our data could sufficiently be explained by phenylsuccinate reducing malate-aspartate-shuttle activity. The shuttle was recently reported to be essential for glucose-derived glutamate production, which is required for the potentiation of GSIS by the gut hormone GLP-1. The hormone-induced cAMP generation was reported to favor glutamate uptake by insulin-containing secretory granules [15].

To conclude, we found that the metabolic response to glucose stimulation was qualitatively similar but quantitatively different in α- (αTC1-6) and ß-cells (INS-1 832/13). The tight coupling between glycolytic and TCA-cycle metabolism in the INS-1 832/13 cells [42] was not observed in the αTC1-6. Metabolism of glucose was still essential for glucose-stimulated glucagon secretion. Inhibition of the malate-aspartate shuttle abolished glucose-stimulated glucagon secretion, whereas GSIS appeared to be partially rescued by compensatory activity in the glycerolphosphate shuttle. Hence, our data suggest that the glycerolphosphate shuttle in the ß-cell allows dose-dependent metabolism of glucose and secretion of insulin at rising concentrations of glucose. A lower expression of this shuttle in the α-cell might prevent hypersecretion of glucagon at hyperglycemia and divert α-cell nutrient sensing from glucose to lactate and pyruvate, metabolites which are increased during physical exercise.

Supplementary Material

Refer to Web version on PubMed Central for supplementary material.

Funding

This work was supported by grants from Swedish Research Council, Novo Nordisk Foundation, Diabetesfonden, the Crafoord, Lars Hierta's Minne, Fredrik och Ingrid Thuring's, O.E. and Edla Johansson's Vetenskapliga, ÅkeWibergs, Direktör Albert Påhlssons, Magnus Bergvalls, and Knut and Alice Wallenberg's Foundations and the Royal Physiographic Society.

Abbreviations

AdipA
adipate

Agc1/Aralar1/Slc25a12
Solute Carrier Family 25 (Aspartate/Glutamate Carrier), Member 12

AKGA
α-ketoglutarate

Europe PMC Funders Author Manuscripts

Ala
alanine

Amal
aminomalonate

Asp
aspartate

Bala
beta-alanine

BenzA
benzoate

C10:0
caproate

C12:0
laurate

C14:0
myristate

C16:0
palmitate

C17:0
heptadecanoate

C18:0
stearate

C18:1
oleate

C20:0
arachidate

C20:4
arachidonate

Chol
cholesterol

Cit
citrate

Creat
creatinine

Europe PMC Funders Author Manuscripts

Ct
cycle threshold

Cys
cysteine

FCS
fetal calf serum

Fruct
fructose

Fruct6P
fructose-6-phosphate

Fum
fumarate

GABA
gamma-aminobutyrate

GLP-1
glucagon-like peptide 1

Glu
glutamate

Gluc6P
glucose-6-phosphate

Gly
glycine

Gly2P
glycerol-2-phosphate

Gly3P
glycerol-3-phosphate

GlyA3P
3-phosphoglycerate

GlycolA
glycolate

Got1
aspartate aminotransferase, cytoplasmic

Gpd1
glycerol-3-phosphate dehydrogenase, cytoplasmic

Europe PMC Funders Author Manuscripts

Gpd2
glycerol-3-phosphate dehydrogenase, mitochondrial

GSIS
glucose stimulated insulin secretion

HBSS
HEPES balanced salt solution

Hk
hexokinase

Hk2
hexokinase 2

Hprt
hypoxanthine phosphoribosyltransferase 1

Ile
isoleucine

InosP
inositolphosphate

IsoCit
isocitrate

Lac
lactate

LDH
lactate dehydrogenase

Lys
lysine

Mal
malate

MCT1
monocarboxylate transporter 1

Meth
methionine

Mino
myo inositol

OCR
oxygen consumption rate

Europe PMC Funders Author Manuscripts

OctOl
octadecanol

OPLS-DA
orthogonal projection to latent structures discriminant analysis

OxalA
oxalate

Pglu
pyruglutamate

Phe
phenylalanine

PhS
phenyl succinate

Pk
pyruvate kinase

Pklr
pyruvate kinase, liver isoform

Pkm2
pyruvate kinase, muscle isoform 2

PMPI
plasma membrane potential indicator

PP
pyrophosphate

Pro
proline

Pyr
pyruvate

QPCR
quantitative real-time PCR

Rib5P
ribose-5-phosphate

Ser
serine

SPAll
all detected hexose phosphates

Succ
succinate

T2D
type 2 diabetes

Tau
taurine

TCA
tricarboxylic acid

Thr
threonine

Ura
uracil

Val
valine

References

1. Kahn SE. The relative contributions of insulin resistance and beta-cell dysfunction to the pathophysiology of Type 2 diabetes. Diabetologia. 2003; 46:3–19. [PubMed: 12637977]
2. Saltiel AR, Kahn CR. Insulin signalling and the regulation of glucose and lipid metabolism. Nature. 2001; 414:799–806. [PubMed: 11742412]
3. Habegger KM, Heppner KM, Geary N, Bartness TJ, DiMarchi R, Tschöp MH. The metabolic actions of glucagon revisited. Nat Rev Endocrinol. 2010; 6:689–697. [PubMed: 20957001]
4. D'Alessio D. The role of dysregulated glucagon secretion in type 2 diabetes. Diabetes Obes Metab. 2011; (Suppl 1):126–132. [PubMed: 21824266]
5. Dunning BE, Gerich JE. The role of alpha-cell dysregulation in fasting and postprandial hyperglycemia in type 2 diabetes and therapeutic implications. Endocr Rev. 2007; 28:253–283. [PubMed: 17409288]
6. Dunning BE, Foley JE, Ahrén B. Alpha cell function in health and disease: influence of glucagon-like peptide-1. Diabetologia. 2005; 48:1700–1713. [PubMed: 16132964]
7. Henquin JC. Triggering and amplifying pathways of regulation of insulin secretion by glucose. Diabetes. 2000; 49:1751–1760. [PubMed: 11078440]
8. Craig TJ, Ashcroft FM, Proks P. How ATP inhibits the open KATP channel. J Gen Physiol. 2008; 132:131–144. [PubMed: 18591420]
9. Rorsman P, Renström E. Insuline granule dynamics in pancreatic beta-cells. Diabetologia. 2003; 46:1029–1045. [PubMed: 12879249]
10. Wiederkehr A, Szanda G, Akhmedov D, Mataki C, Heizmann CW, Schoonjans K, Pozzan T, Spät A, Wollheim CB. Mitochondrial matrix calcium is an activating signal for hormone secretion. Cell Metab. 2011; 13:601–611. [PubMed: 21531342]
11. Watkins DT, Moore M. Uptake of NADPH by islet secretion granule membranes. Endocrinology. 1977; 100:1461–1467. [PubMed: 14821]
12. Ivarsson R, Quintens R, Dejonghe S, Tsukamoto K, in t Veld P, Renström E, Schuit FC. Redox control of exocytosis: regulatory role of NADPH, thioredoxiin, and glutaredoxin. Diabetes. 2005; 54:2132–2142. [PubMed: 15983215]
13. Maechler P, Wollheim CB. Mitochondrial glutamate acts as a messenger in glucose-induced insulin exocytosis. Nature. 1999; 402:685–689. [PubMed: 10604477]

14. Feldmann N, del Rio RM, Gjinovci A, Tamarit-Rodriguez J, Wollheim CB, Wiederkehr A. Reduction of plasma membrane glutamate transport potentiates insulin but not glucagon secretion in pancreatic islet cells. Mol Cell Endocrinol. 2011; 338:46–57. [PubMed: 21371522]
15. Gheni G, Ogura M, Iwasaki M, Yokoi N, Minami K, Kakayama Y, Harada K, Hastoy B, Wu X, Takahashi H, Kimura K, et al. Glutamate acts as a key signal linking glucose metabolism to incretin/cAMP action to amplify insulin secretion. Cell Reports. 2014; 9:661–673. [PubMed: 25373904]
16. Ashcroft FM, Rorsman P. Diabetes mellitus and the beta-cell: the last ten years. Cell. 2012; 148:148–156.
17. Ashcroft FM, Harrison DE, Ashcroft SJ. Glucose induces closure of single potassium channels in isolated rat pancreatic beta-cells. Nature. 1984; 312:446–448. [PubMed: 6095103]
18. Olsen HL, Theander S, Bokvist K, Buschard K, Wollheim CB, Gromada J. Glucose stimulates glucagon release in single rat alpha-cells by mechanisms that mirror the stimulus secretion coupling in beta-cells. Endocrinology. 2005; 146:4861–4870. [PubMed: 16081632]
19. Le Marchand SJ, Piston DW. Glucose supression of glucagon secretion: Metabolic and calcium responses from alpha-cells in intact mouse pancreatic islets. J Biol Chem. 2010; 285:14389–14398. [PubMed: 20231269]
20. Franklin I, Gromada J, Gjinovci A, Theander S, Wollheim CB. Beta-cell secretory products activate alpha-cell ATP-dependent potassium channels to inhibit glucagon release. Diabetes. 2005; 54:1808–1815. [PubMed: 15919803]
21. Ravier MA, Rutter GA. Glucose or insulin, but not zink ions, inhibit glucagon secretion from mouse pancreatic alpha-cells. Diabetes. 2005; 54:1789–1797. [PubMed: 15919801]
22. Ishihara H, Maechler P, Gjinovci A, Herrera P-L, Wollheim CB. Islet beta-cell secretion determines glucagon release from neighbouring alpha-cells. Nat Cell Biol. 2003; 5:330–335. [PubMed: 12640462]
23. Gromada J, Franklin I, Wollheim CB. Alpha-cells of the endocrine pancreas: 35 years of research but the enigma remains. Endocr Rev. 2007; 28:84–116. [PubMed: 17261637]
24. Rorsman P, Ramracheya R, Rorsman NJ, Zhang Q. ATP-regulated potassium channels and voltage-gated calcium channels in pancreatic alpha and beta cells: similar functions but reciprocal effects on secretion. Diabetologia. 2014; 57:1749–1761. [PubMed: 24906950]
25. Zou N, Wu X, Jin YY, He MZ, Wang XX, Su LD, Rupnik M, Wu ZY, Liang L, Shen Y. ATP regulates sodium channel kinetics in pancreatic islet beta cells. J Membr Biol. 2013; 246:101–107. [PubMed: 23296347]
26. Göpel SO, Kanno T, Barg S, Rorsman P. Patch-clamp characterisation of somatostatin-secreting cells in intact mouse pancreatic islets. J Physiol. 2000; 528:497–507. [PubMed: 11060127]
27. Göpel SO, Kanno T, Barg S, Weng XG, Gromada J, Rorsman P. Regulation of glucagon release in mouse cells by KATP channels and inactivation of TTX-sensitive Na+ channels. J Physiol. 2000; 528:509–520. [PubMed: 11060128]
28. Zhang Q, Ramracheya R, Lahmann C, Tarasov A, Bengtsson M, Braha O, Braun M, Brereton M, Collins S, Galvanosvskis J, Gonzalez A, et al. Role of Katp channels in glucose-regulated glucagon secretion and impaired counterregulation in type 2 diabetes. Cell Metab. 2013; 18:871–882. [PubMed: 24315372]
29. Ramracheya R, Ward C, Shigeto M, Walker JN, Amisten S, Zhang Q, Johnson PR, Rorsman P, Braun M. Membrane potential-dependent inactivation of voltage-gated ion channels in alpha-cells inhibits glucagon secretion from human islets. Diabetes. 2010; 59:2198–2208. [PubMed: 20547976]
30. Braun M, Ramracheya R, Bengtsson M, Zhang Q, Karanauskaite J, Partridge C, Johnson PR, Rorsman P. Voltage-gated ion channels in human pancreatic beta-cells: electrophysiological characterization and role in insulin secretion. Diabetes. 2008; 57:1618–1628. [PubMed: 18390794]
31. Müller WA, Faloona GR, Aguilar-Parada E, Unger RH. Abnormal alpha-cell function in diabetes: Response to carbohydrate and protein ingestion. N Engl J Med. 1970; 283:109–115. [PubMed: 4912452]
32. Salehi A, Vieira E, Gylfe E. Paradoxical stimulation of glucagon secretion by high glucose concentrations. Diabetes. 2006; 55:2318–2323. [PubMed: 16873696]

33. Vieira E, Salehi A, Gylfe E. Glucose inhibits glucagon secretion by a direct effect on mouse pancreatic alpha cells. Diabetologia. 2007; 50:370–379. [PubMed: 17136393]
34. Reimann F, Habib AM, Tolhurst G, Parker HE, Rogers GJ, Gribble FM. Glucose sensing in L-cells: a primary cell study. Cell Metab. 2008; 8:447–449. [PubMed: 19041758]
35. Spégel P, Malmgren S, Sharoyko VV, Newsholme P, Koeck T, Mulder H. Metabolomic analyses reveal profound differences in glycolytic and tricarboxylic acid cyclen metabolism in glucose-responsive and -unresponsive clonal beta-cell lines. Biochem J. 2011; 435:277–284. [PubMed: 21208194]
36. Spégel P, Sharoyko VV, Goehring I, Danielsson APH, Malmgren S, Nagorny CLF, Andersson LE, Koeck T, Sharp GWG, Straub SG, Wollheim CB, et al. Time resolved metabolomics analysis of beta-cells implicates the pentose phosphate pathway in the control of insulin release. Biochem J. 2013; 450:595–605. [PubMed: 23282133]
37. Jonsson P, Sjövik Johansson E, Wuolikainen A, Lindberg J, Shuppe-Koistinen I, Kusano M, Sjöström M, Trygg J, Moritz T, Antti H. Predictive metabolite profiling applying hierchal multivariate curve resolution to GC-MS data - A potential tool for multi-parametric diagnosis. J Proteome Res. 2006; 5:1407–1414. [PubMed: 16739992]
38. Goehring I, Sharoyko VV, Malmgren S, Andersson LE, Spégel P, Nicholls D, Mulder H. Chronic high glucose and pyruvate levels differentially affect mitochondrial bioenergetics and fuel-stimulated insulin secretion from clonal INS-1 832/13 cells. J Biol Chem. 2013; 289:3786–3798. [PubMed: 24356960]
39. Nicholls DG. Simultaneous monitoring of ionophore- and inhibitor-mediated plasma and mitochondrial membrane potential changes in cultured neurons. J Biol Chem. 2006; 281:14864–14874. [PubMed: 16551630]
40. Krus U, Kotova O, Spégel P, Hallgard E, Vedin A, Moritz T, Sugden MC, Koeck T, Mulder H. Pyruvate dehydrogenase kinase 1 controls mitochondrial metabolism and insulin secretion in INS-1 832/13 clonal β-cells. Biochem J. 2010; 429:205–213. [PubMed: 20415663]
41. Hirose H, Lee YH, Inman LR, Nagasawa Y, Johnson JH, Unger RH. Defective fatty acid-mediated beta-cell compensation in Zucker diabetic fatty rats: Pathogenic implications for obesity-dependent diabetes. J Biol Chem. 1996; 271:5633–5637. [PubMed: 8621426]
42. Malmgren S, Nicholls DG, Taneera J, Bacos K, Koeck T, Tamaddon A, Wibom R, Groop L, Ling C, Mulder H, Sharoyko VV. Tight coupling between glucose and mitochondrial metabolism in clonal beta-cells is required for robust insulin secretion. J Biol Chem. 2009; 284:32395–32404. [PubMed: 19797055]
43. Trygg J, Wold S. Orthogonal projections to latent structures (O-PLS). J Chemom. 2002; 16:119–128.
44. Kim A, Miller K, Jo J, Kilimnik G, Wojcik P, Hara M. Islet architecture: A comparative study. Islets. 2009; 1:129–136. [PubMed: 20606719]
45. Hamaguchi K, Leiter EH. Comparision of cytokine effects on mouse pancreatic alpha-cell and beta-cell lines: Viability, secretory function, and MHC antigen expression. Diabetes. 1990; 39:414–425.
46. Hohmeier HE, Mulder H, Chen G, Henkel-Rieger R, Prentki M, Newgard CB. Isolation of INS-1-derived cell lines with robust ATP-sensitive K+ channel-dependent and - independent glucose-stimulated insulin secretion. Diabetes. 2000; 49:424–430. [PubMed: 10868964]
47. Detimary P, Dejonghe S, Ling Z, Pipeleers D, Schuit F, Henquin JC. The changes in adenine nucleotides measured in glucose-stimulated rodent islets occur in beta cells but not in alpha cells and are also observed in human islets. J Biol Chem. 1998; 273:33905–33908. [PubMed: 9852040]
48. Quesada I, Todorova MG, Soria B. Different metabolic responses in alpha-, beta-, and delta-cells of the islet of Langerhans monitored by redox confocal microscopy. Biophys J. 2006; 90:2641–2650. [PubMed: 16399832]
49. Schuit F, De Vos A, Farfari S, Moens K, Pipeleers D, Brun T, Prentki M. Metabolic fate of glucose i purified islet cells - Glucose-regulated anaplerosis in beta-cells. J Biol Chem. 1997; 272:18572–18579. [PubMed: 9228023]

50. Bender K, Newsholme P, Brennan L, Maechler P. The importance of redox shuttles to pancreatic beta-cell energy metabolism and function. Biochem Soc Trans. 2006; 34:811–814. [PubMed: 17052204]
51. Eto K, Tsubamoto Y, Terauchi Y, Sugiyama T, Kishimoto T, Takahashi N, Yamauchi N, Kubota N, Murayama S, Aizawa T, Akanuma Y, et al. Role of NADH shuttle system in glucose-induced activation of mitochondrial metabolism and insulin secretion. Science. 1999; 283:981–985. [PubMed: 9974390]
52. McKenna MC, Waagepetersen HS, Schousboe A, Sonnewald U. Neuronal and astrocytic shuttle mechanisms for cytosolic-mitochondrial transfer of reducing equivalents: current evidence and pharmacological tools. Biochem Pharmacol. 2006; 71:399–407. [PubMed: 16368075]
53. Odegaard ML, Joseph JW, Jensen MV, Lu D, Ilkayeva O, Ronnebaum SM, Becker TC, Newgard CB. The mitochondrial 2-oxoglutarate carrier is part of a metabolic pathway that mediates glucose- and glutamine-stimulated insulin secretion. J Biol Chem. 2010; 285:16530–16537. [PubMed: 20356834]
54. Sekine N, Vincenzo C, Romano R, Brown LJ, Gine E, Tamarit-Rodriguez J, Girotti M, Marie S, MacDonald MJ, Wollheim CB, Rutter GA. Low lactate dehydrogenase and high mitochondrial glycerol phosphate dehydrogenase in pancreatic beta-cells. J Biol.Chem. 1994; 269:4895–4902. [PubMed: 8106462]
55. Ishihara H, Wang H, Drewes LR, Wollheim CB. Overexpression of monocarboxylate transporter and lactate dehydrogenase alters insulin secretory responses to pyruvate and lactate in beta-cells. J Clin Invest. 1999; 104:1621–1629. [PubMed: 10587526]
56. Wiederkehr A, Wollheim CB. Mitochondrial signals drive insulin secretion in the pancreatic beta-cell. Mol Cell Endocrinol. 2012; 353:128–137. [PubMed: 21784130]
57. Rubi B, del Arco A, Bartley C, Satrustegui J, Maechler P. The Malate-Aspartate NADH Shuttle Member Aralar1 Determines Glucose Metabolic Fate, Mitochondrial Activity, and Insulin Secretion in Beta Cells. J Biol Chem. 2004; 279:55659–55666. [PubMed: 15494407]
58. Quintens R, Hendrickx N, Lemaire K, Schuit F. Why expression of some genes is disallowed in beta-cells. Biochem Soc Trans. 2008; 36:300–305. [PubMed: 18481946]
59. Giroix MH, Rasschaert J, Bailbe D, Leclercq-Meyer V, Sener A, Portha B, Malaisse WJ. Impairment of glycerol phosphate shuttle in islets from rats with diabetes induced by neonatal streptozocin. Diabetes. 1991; 40:227–232. [PubMed: 1825072]
60. Östenson C-G, Abdel-Halim SM, Rasschaert J, Malaisse-Lagae E, Meuris S, Sener A, Efendic S, Malaisse WJ. Deficient activity of FAD-linked glycerophosphate dehydrogenase in islets of GK rats. Diabetologia. 1993; 36:722–726. [PubMed: 8405739]
61. Malaisse WJ. Is type 2 diabetes due to a deficiency of FAD-linked glycerophosphate dehydrogenase in pancreatic islets? Acta Diabetol. 1993; 30:1–5. [PubMed: 8329724]
62. Koza RA, Kozak UC, Brown LJ, Leiter EH, MacDonald MJ, Kozak LP. Sequence and tissue-dependent RNA expression of mouse FAD-linked glycerol-3-phosphate dehydrogenase. Arch Biochem Biophys. 1996; 336:97–104. [PubMed: 8951039]
63. MacDonald MJ. High content of mitochondrial glycerol-3-phosphate dehydrogenase in pancreatic islets and its inhibition by diazoxide. J Biol Chem. 1981; 256:8287–8290. [PubMed: 6790537]
64. Anunciado-Koza R, Ukropec J, Koza RA, Kozak LP. Inactivation of UCP1 and the glycerol phosphate cycle synergistically increases energy expenditure to resist diet-induced obesity. J Biol Chem. 2008; 283:27688–27697. [PubMed: 18678870]
65. Marliss EB, Wollheim CB, Blondel B, Orci L, Lambert AE, Stauffacher W, Like AA, Renold AEB. Insulin and glucagon release from monolayer cell cultures of pancreas from newborn rats. Eur J Clin Invest. 1973; 3:16–26. [PubMed: 4569080]
66. Wasserman K, Beaver WL, Davis JA, Pu JZ, Heber D, Whipp BJ. Lactate, pyruvate, and lactate-to-pyruvate ratio during exercise and recovery. J Appl Physiol. 1985; 59:935–940. [PubMed: 4055579]
67. Hoy M, Maechler P, Efanov AM, Wollheim CB, Berggren PO, Gromada J. Increase in cellular glutamate levels stimulates exocytosis in pancreatic beta-cells. FEBS Lett. 2002; 531:199–203. [PubMed: 12417312]

68. MacDonald MJ, Fahien LA. Glutamate Is Not a Messenger in Insulin Secretion. J Biol Chem. 2000; 275:34025–34027. [PubMed: 10967090]

69. Jaques F, Jousset H, Thomas A, Prost AL, Wollheim CB, Irnminger JC, Demaurex N, Halban PA. Dual effect of cell-cell contact disruption on cytosolic calcium and insulin secretion. Endocrinology. 2008; 149:2494–2505. [PubMed: 18218692]

70. Skelin M, Rupnik M, Cencic A. Pancreatic beta cell lines and their applications in diabetes mellitus research. ALTEX. 2010; 27:105–113. [PubMed: 20686743]

71. Passarella S, Atlante A, Barile M, Quagliariello E. Anion transport in rat brain mitochondria: Fumarate uptake via the dicarboylate carrier. Neurochem Res. 1987; 12:255–264. [PubMed: 3587497]

72. Arsenian M. Potential cardiovascular applications of glutamate, aspartate, and other amino acids. Clin Cardiol. 1998; 21:620–624. [PubMed: 9755377]

Europe PMC Funders Author Manuscripts

Europe PMC Funders Author Manuscripts

Summary statement

Secretion of both glucagon and insulin is perturbed in Type 2 diabetes. Here, we identify a difference in mitochondrial shuttling between α- and β-cells that adjusts nutrient sensing and which potentially could be employed to specifically target secretion of either hormone.

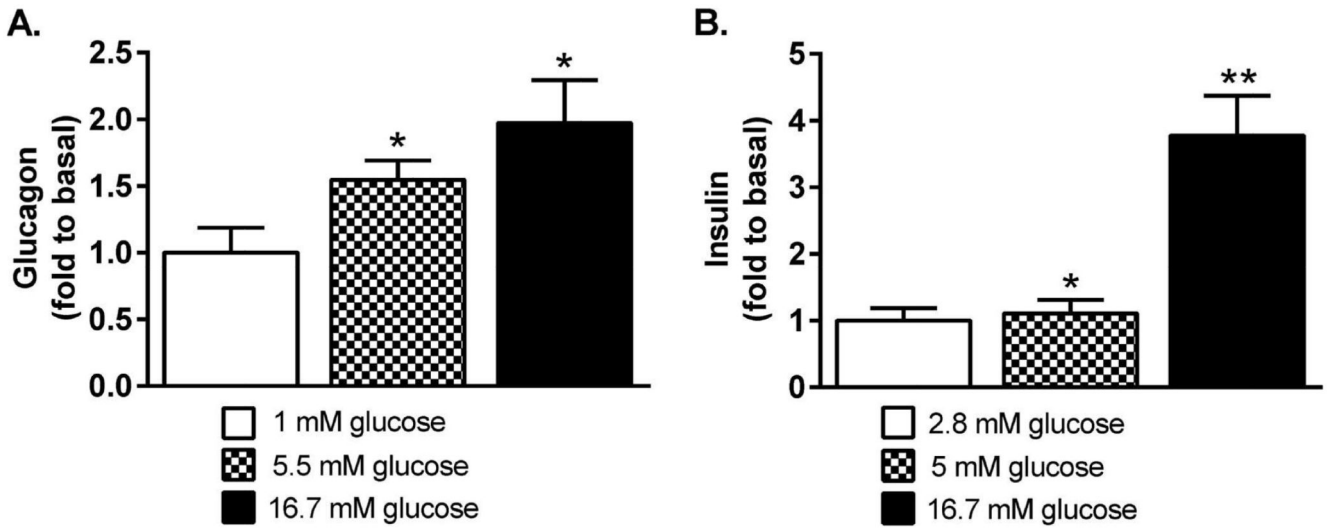

Figure 1. Glucose dose-dependently provokes hormone secretion from αTC1-6 and INS-1 832/13 cells

(A) Glucagon secretion from the αTC1-6 cell line and **(B)** insulin secretion from the INS-1 832/13 cell line increase with glucose concentration. Data are expressed as mean normalized to basal secretion at 1 mM glucose (A) and 2.8 mM glucose (B) for n=12 (A) and n=6 (B). Statistical significance was assessed using the paired Student´s t-test, *p<0.05, **p<0.01.

Europe PMC Funders Author Manuscripts

Europe PMC Funders Author Manuscripts

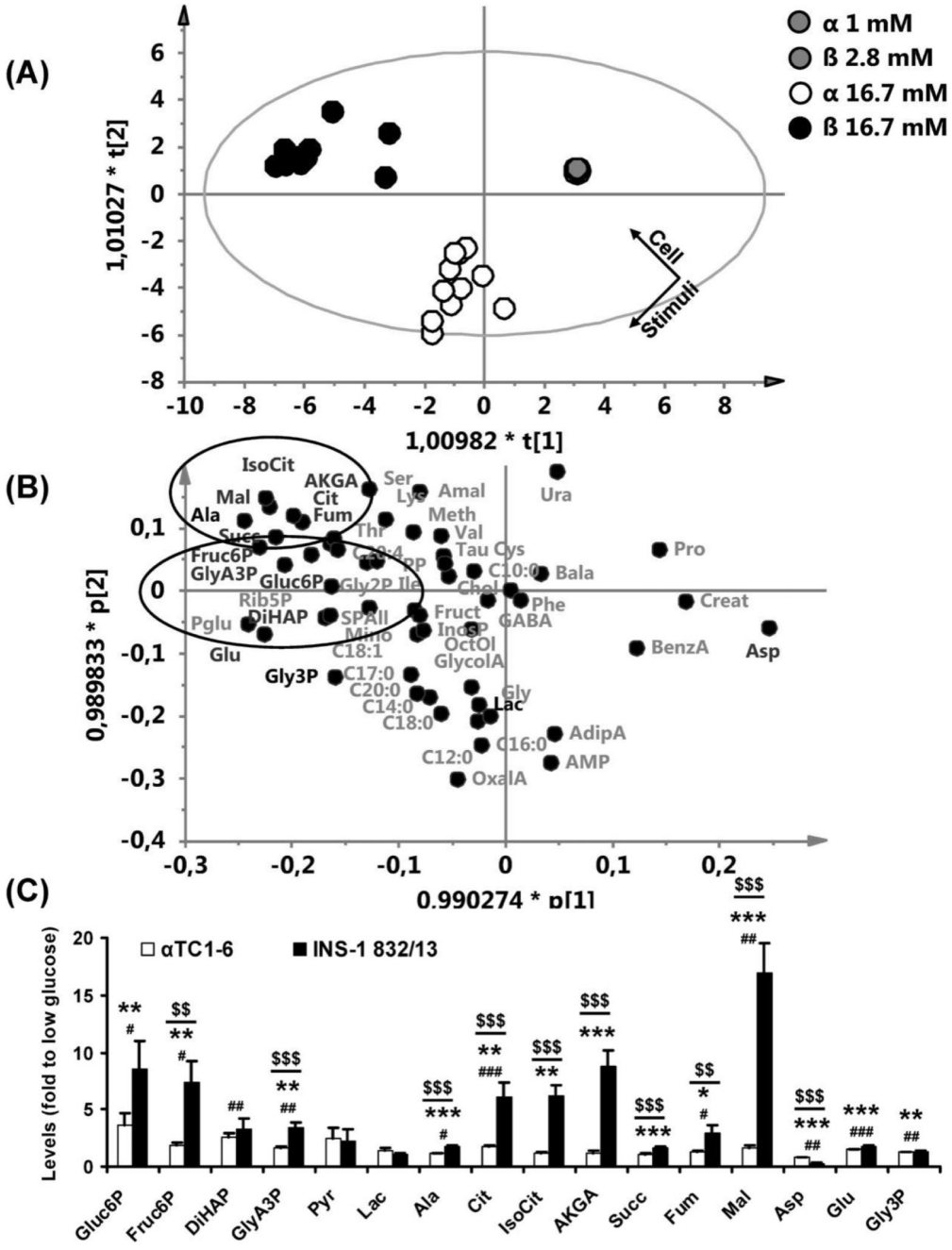

Figure 2. Levels of TCA-cycle intermediates are less glucose responsive in αTC1-6 than in INS-1 832/13

(A) A score-scatter plot for an OPLS-DA calculated with the cell-type (αTC1-6 or INS-1 832/13) and the stimulatory glucose level as discriminating variables. Each point in this plot corresponds to a sample; the position of the point is determined by levels of all detected metabolites. **(B)** The loading-scatter plot corresponding to the score-scatter plot shown in (A) reveals which changes in metabolite levels that underlie the clustering of samples observed in (A). **(C)** Fold-changes in metabolite levels after stimulation of αTC1-6 and

INS-1 832/13-cells with 16.7 mM glucose. Data are shown for αTC1-6 (n=12) and INS-1 832/13 (n=11) in (A-C), expressed as the average fold-change to basal glucose levels ± SEM in (C). Statistical significance was assessed using ANOVA and the paired (within cell-type) and unpaired (between cell-types) Student's t-test. 2.8 vs 16.7 mM glucose for INS-1 832/13, *p<0.05, **p<0.01, ***p<0.001. 1 vs 16.7 mM glucose for αTC1-6, #p<0.05, ##p<0.01, ###p<0.001. Fold-change for αTC1-6 vs INS-1 832/13, $$p<0.01, $$$p<0.001. First (t[1]) and second (t[2]) predictive component; first (p[1]) and second (p[2]) predictive loadings scaled as correlations. Glycolytic and TCA-cycle intermediates are indicated by ellipses. Metabolites discussed in the text are shown in black, additional metabolites are shown in grey. Mal, malate; Fum, fumarate; Cit, citrate; IsoCit, isocitrate; Succ, succinate; AKGA, α-ketoglutarate; Ala, alanine; Pyr, pyruvate; Lac, lactate; Gluc6P, glucose-6-phosphate; Fruct6P, fructose-6-phosphate; GlyA3P, 3-phosphoglycerate; Gly3P, glycerol-3-phosphate; Asp, aspartate; Glu, glutamate; Rib5P, ribose-5-phosphate; Pglu, pyruglutamate; Ser, serine; Lys, lysine; Thr, threonine; Gly2P, glycerol-2-phosphate; Amal, aminomalonate; Meth, methionine; Val, valine; Tau, taurine; PP, pyrophosphate; Ile, isoleucine; Cys, cysteine; Chol, cholesterol; Ura, uracil; Bala, beta-alanine; Pro, proline; SPAll, all detected hexose phosphates; Mino, myo inositol; Fruct, fructose; InosP, inositolphosphate; OctOl, octadecanol; GlycolA, glycolate; OxalA, oxalate; GABA, gamma-aminobutyrate; Phe, phenylalanine; Gly, glycine; Creat, creatinine; BenzA, benzoate; AdipA, adipate; C10:0, caproate; C12:0, laurate; C14:0, myristate; C16:0, palmitate; C17:0, heptadecanoate; C18:0, stearate; C18:1, oleate; C20:0, arachidate; C20:4, arachidonate.

Europe PMC Funders Author Manuscripts

Europe PMC Funders Author Manuscripts

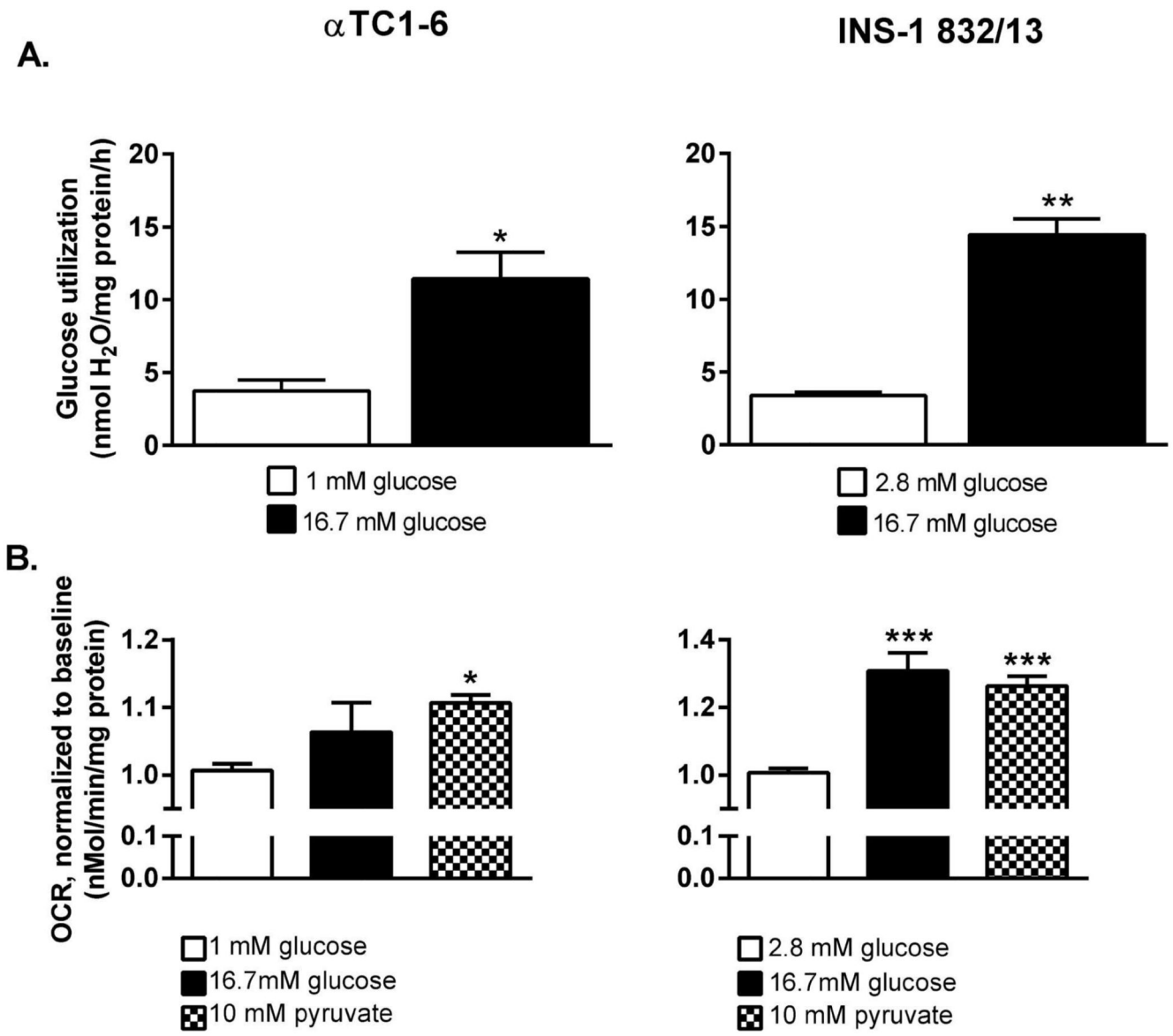

Figure 3. The coupling between glycolytic and mitochondrial glucose oxidation is more efficient in the INS-1 832/13 than in the αTC1-6 cell line

(A) Glucose utilization increase in αTC1-6 cells and INS-1 832/13 cells stimulated with 16.7 mM glucose. **(B)** Oxygen consumption rate (OCR) in the αTC1-6 cell line and the INS-1 832/13 cells after stimulation with 16.7 mM glucose and 10 mM pyruvate. OCR was measured first at 1 mM (αTC1-6) or 2.8 mM (INS-1 832/13) glucose (baseline) followed by measurements after injection of 16.7 mM glucose or 10 mM pyruvate. Data are expressed as mean ± SEM for n=3 (A), n=3 (10 mM pyruvate and 16.7 mM glucose for αTC1-6 in B), n=5 (16.7 mM glucose for INS-1 832/13 in B), n=8 (baseline INS-1 832/13), and n=6 (baseline αTC1-6). Statistical significance was assessed by the Student´s t-test (A) and ANOVA followed by the Newman-Keuls multiple correction method *post hoc* (B); *p<0.05, **p<0.01, ***p<0.001.

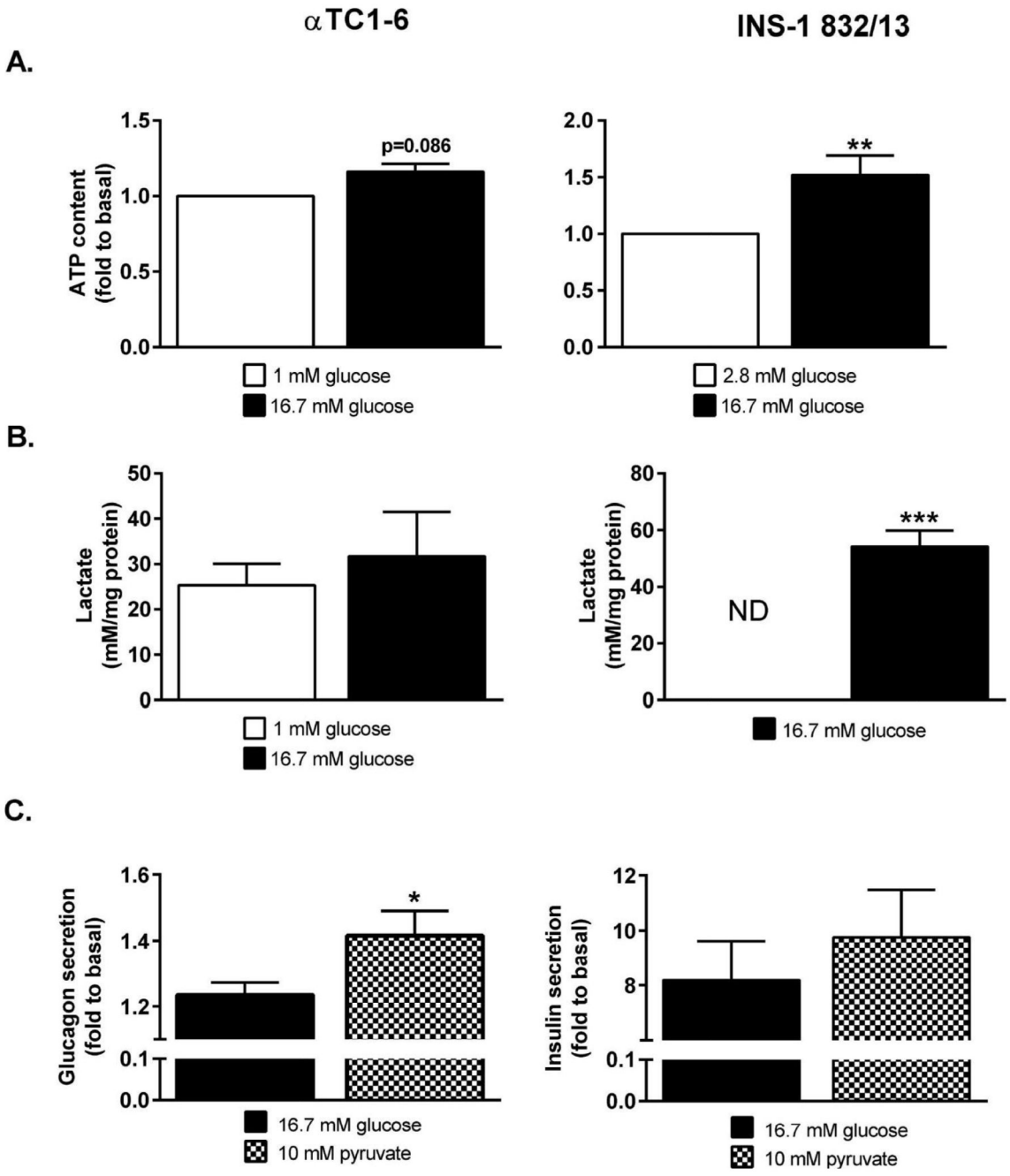

Figure 4. ATP-levels and lactate release are largely glucose-unresponsive in αTC1-6 cells whereas they increase in INS-1 832/13 cells stimulated with 16.7 mM glucose

(A) ATP content in αTC1-6 stimulated with 1 or 16.7 mM glucose and INS-1 832/13 cells stimulated with 2.8 or 16.7 mM glucose. **(B)** Lactate release from αTC1-6 stimulated with 1 or 16.7 mM glucose and INS-1 832/13 cells stimulated with 2.8 or 16.7 mM glucose. **(C)** Glucagon secretion from the αTC1-6 cells and insulin secretion from INS-1 832/13 cells stimulated with 16.7 mM glucose or 10 mM pyruvate. Data are expressed as means normalized to levels at 1 mM (αTC1-6, A) and 2.8 mM (INS-1 832/13, A) glucose ± SEM

for n=6 (αTC1-6, A), n=10 (INS-1 832/13, A), n=3 (αTC1-6, B), n=4 (INS-1 832/13, B), n=6 (10 mM pyruvate, INS-1 832/13, C), n=3 (16.7 mM glucose, INS-1 832/13, C), and n=4 (αTC1-6, C). Statistical significance was assessed using the paired Student´s t-test, *$p<0.05$. ND; below detection limit.

Europe PMC Funders Author Manuscripts

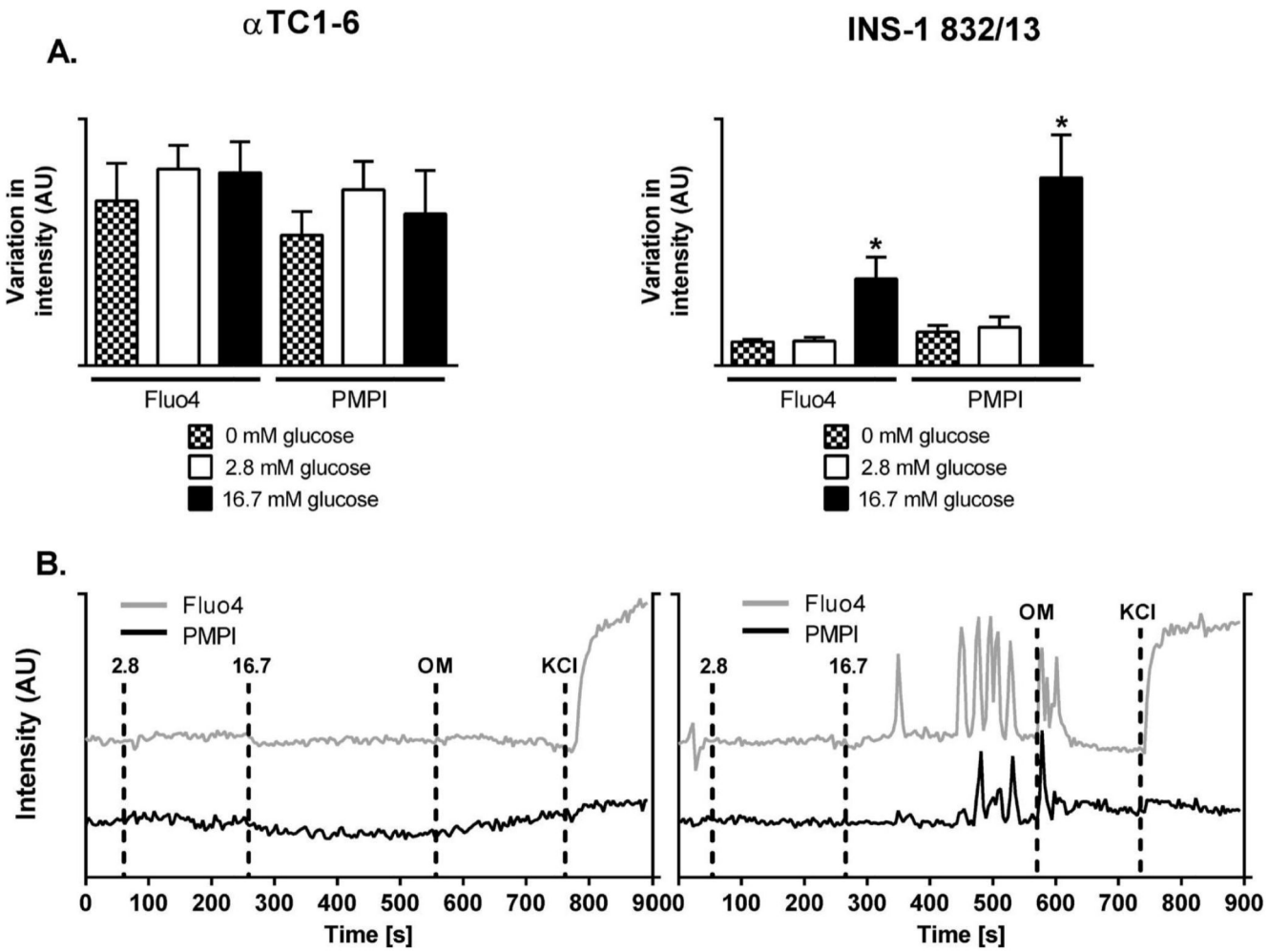

Figure 5. Glucose elicits strong responses in plasma membrane potential and Ca^{2+}-fluxes in the INS-1 832/13 cells

(A) Plasma membrane potential oscillations and Ca^{2+}-fluxes expressed as standard deviations in αTC1-6 and INS-1 832/13 cells at 0, 2.8, and 16.7 mM glucose. **(B)** Representative traces for αTC1-6 cells and INS-1 832/13 cells; markers: 2.8-2.8 mM glucose, 16.7-16.7 mM glucose, OM-0.5 ng/μl Oligomycin, KCl-25 mM KCl. Data in (A) are expressed as mean standard deviation for the traces corresponding to the respective glucose level± SEM for n=7.

Europe PMC Funders Author Manuscripts

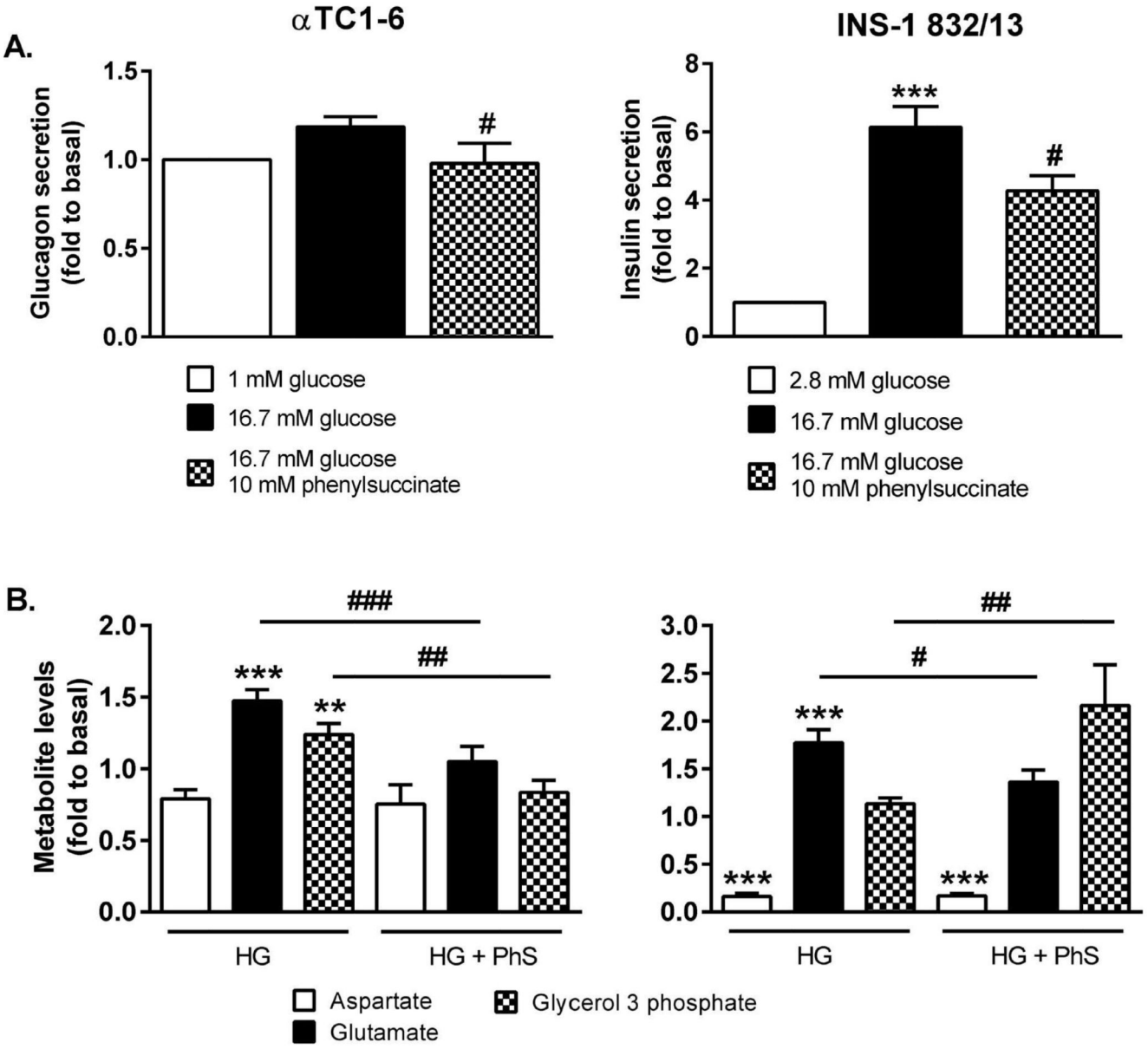

Figure 6. Inhibition of the 2-oxoglutarate carrier abolishes glucose-stimulated glucagon secretion from αTC1-6 cells and reduces glucose-stimulated insulin secretion from INS-1 832/13 cells

(A) Glucagon secretion from the αTC1-6 cells and insulin secreton from INS-1 832/13 cells upon inhibition of the 2-oxoglutarate transporter with 10 mM phenylsuccinate. **(B)** Glucose-evoked alterations in shuttle intermediates in αTC1-6 and INS-1 832/13 cells treated with 10 mM phenylsuccinate. Data is expressed as means normalized to levels at 1 mM glucose (αTC1-6) and 2.8 mM glucose (INS-1 832/13) ± SEM for n=12 (1 mM and 16.7 mM glucose, αTC1-6), n=4 (16.7 mM glucose + 10 mM phenylsuccinate, αTC1-6), and n=8 (INS-1 832/13). Statistical significance was assessed using ANOVA followed by Newman-Keuls multiple comparison test post hoc, baseline vs 16.7 mM glucose *p<0.05, ***p<0.001, 16.7 mM glucose vs 16.7 mM glucose + phenylsuccinate, #p<0.05, ##p<0.01.

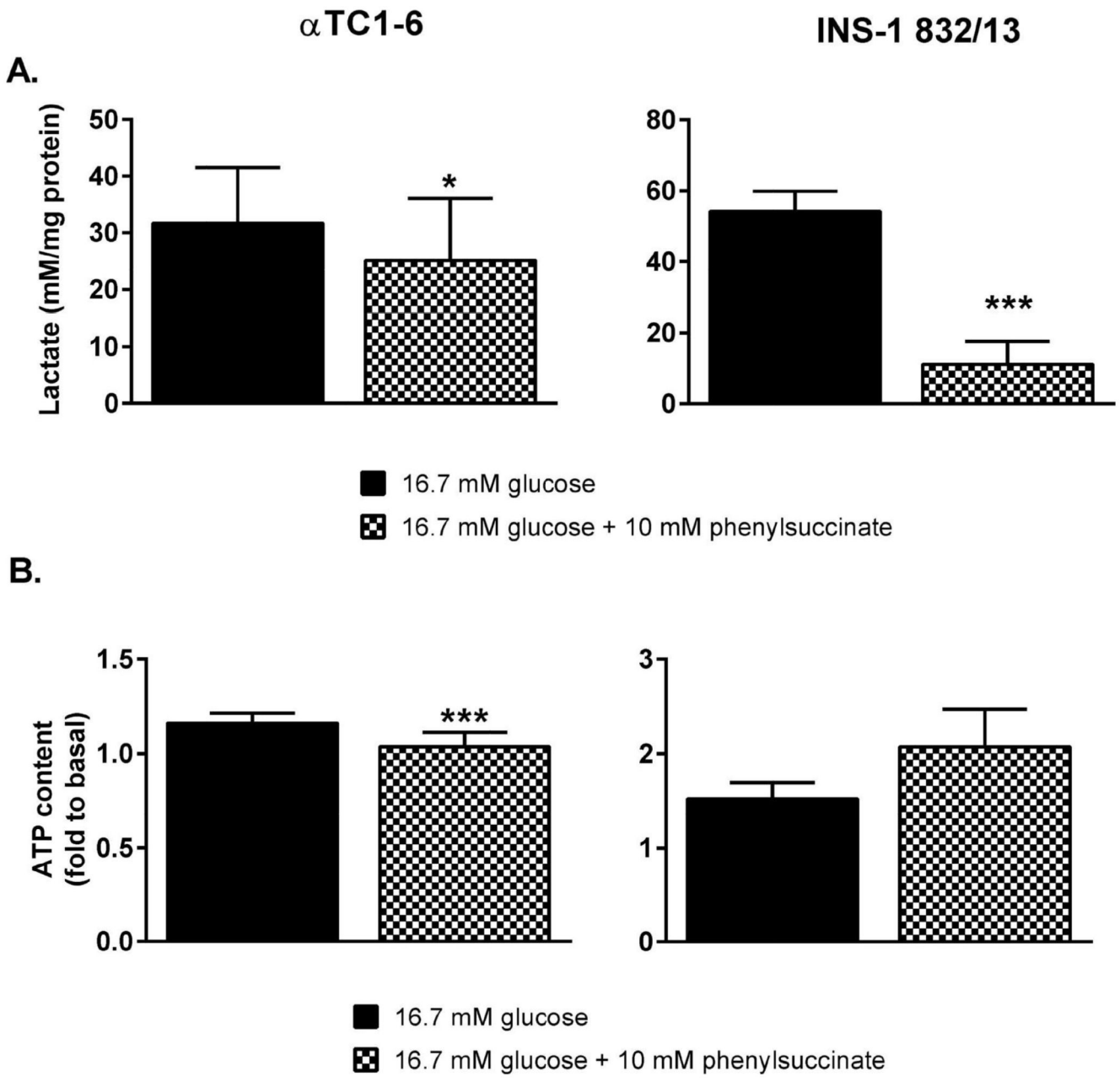

Figure 7. Inhibition of the 2-oxoglutarate carrier with phenylsuccinate abolishes glucose-elicited respiration and ATP-production in αTC1-6 cells but is without effect on OCR and ATP-production in INS-1 832/13 cells

(A) Glucose provoked lactate release from αTC1-6 and INS-1 832/13 cells in the presence of 10 mM phenylsuccinate. **(B)** ATP levels in αTC1-6 and INS-1 832/13 cells treated with 10 mM phenylsuccinate. Data are expressed as means (A) normalized to 1 mM (αTC1-6, B) and 2.8 mM (INS-1 832/13, B) glucose ± SEM for n=3 (αTC1-6, A), n=4 (INS-1 832/13, A), n=6 (αTC1-6, B), n=10 (16.7 mM glucose, INS-1 832/13, B), and n=4 (16.7 mM glucose + 10 mM phenylsuccinate, INS-1 832/13, B). Statistical significance was assessed by the paired Student's t-test, *$p<0.05$, ***$p<0.001$.

Europe PMC Funders Author Manuscripts

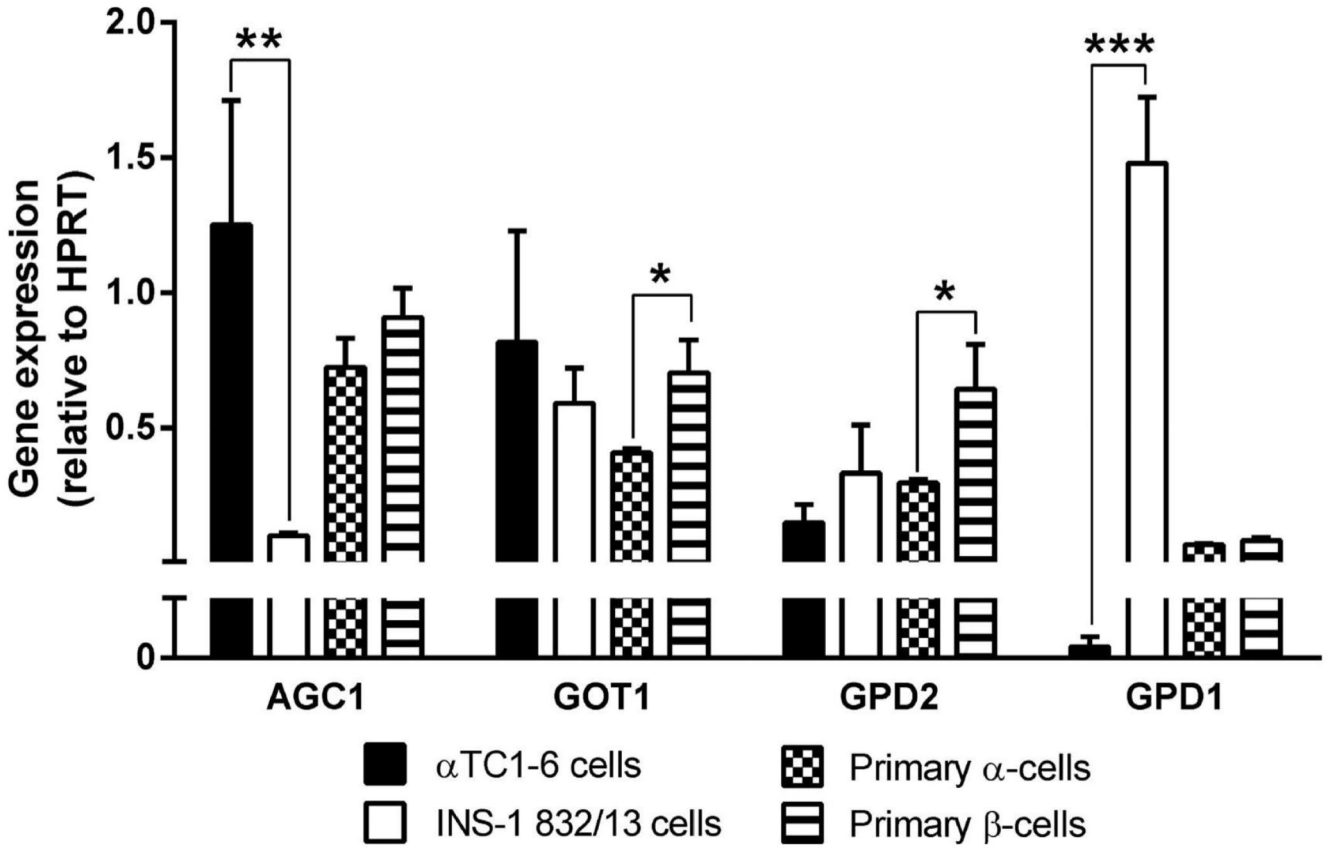

Figure 8. Expression of glycerol-3-phosphate dehydrogenase, the rate limiting enzyme of the glycerol-phosphate shuttle, is lower in αTC1-6- and primary α-cells compared to in INS-1 832/13- and primary ß-cells

Expression levels of genes in the malate-aspartate and glycerolphosphate shuttles in αTC1-6, INS-1 832/13, and primary α- and ß-cells. Data are expressed as means normalized to *Hprt1* ± SEM for n=3. Statistical significance was assessed by the Student's t-test, *p<0.05, **p<0.01, ***p<0.001. *Agc1*, mitochondrial aspartate/glutamate carrier *Aralar1* (*Slc25a12*); *Got1*, cytosolic aspartate amino transferase; *Gpd2*, mitochondrial glycerol-3-phosphate dehydrogenase; *Gpd1*, cytosolic glycerol-3-phosphate dehydrogenase.

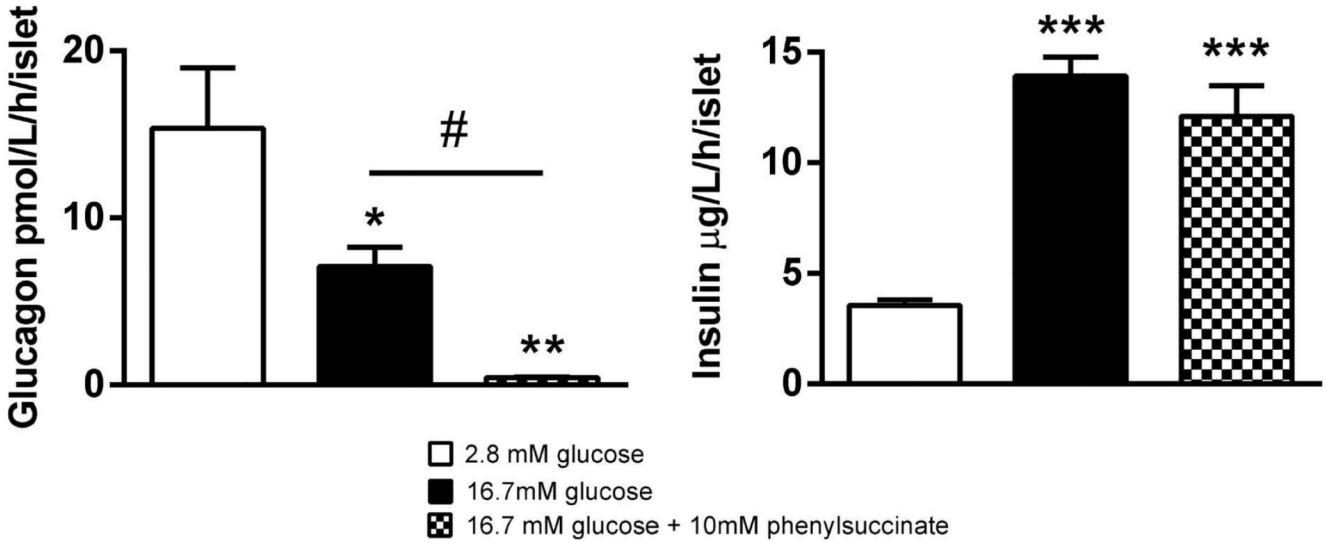

Figure 9. Glucose-stimulated insulin secretion from mouse islets is unaffected by phenylsuccinate, whereas glucagon secretion is abolished

Insulin and glucagon secretion from mouse islets after stimulation with 2.8 or 16.7 mM glucose in the presence or absence of phenylsuccinate. Data are expressed as means ± SEM for n=4. Statistical significance was assesed by ANOVA followed by Newman-Keuls multiple comparison test post hoc. *p<0.05, **p<0.01, ***p<0.001 versus 2.8 mM glucose. #p<0.05 versus indicated condition.

Europe PMC Funders Author Manuscripts